1-1-2017

The Role Of Line-1 Transposable Element In Methamphetamine Neurotoxicity In The Neurogenic Zones

Dongyue Yu
Wayne State University,

THE ROLE OF LINE-1 TRANSPOSABLE ELEMENT IN METHAMPHETAMINE NEUROTOXICITY IN THE NEUROGENIC ZONES

by

DONGYUE YU

THESIS

Submitted to the Graduate School

Wayne State University,

Detroit, Michigan

In partial fulfillment of the requirements

for the degree of

MASTER OF SCIENCE

2017

MAJOR: PHARMACEUTICAL SCIENCES

Approved By:

_____

Advisor Date

Date

DEDICATION

For Minghua Yu and Wei Zhou, who love me.

For Wenjie Yu, Xiulan Wen and Jiaping Mu, who love me too.

“The truth. It is a beautiful and terrible thing, and should, therefore, be treated with great caution.”

---Prof. Dumbledore

ACKNOWLEDGMENTS

Foremost, I would like to express my sincere gratitude to my advisor, Dr. Anna Moszczynska, for all the guidance, patience and encouragement that she provided throughout the duration of this project. Thank you so much for standing by me all the time. I could not have imagined having a better advisor and mentor for my Master's degree study.

I'm also very grateful to my other thesis committee members, Dr. Fei Chen and Dr. Kyle Burghardt, for their encouragement, insightful comments, and constructive criticisms.

I would like to further extend my sincerest thanks and appreciation to Dr. Amanda Flack, Dr. Sean Callan, Yao Fu, Akhil Sharma, and Arman Harutyunyan for their help, support and encouragement.

Last but not least, I would like to thank all my friends, who make my world magical.

TABLE OF CONTENTS

LIST OF FIGURES

ABBREVIATIONS

METH – Methamphetamine

LINE-1 - Long interspersed element 1

TEs - Transposable elements

DNA - Deoxyribonucleic acid

GABA - Gamma amino butyric acid

SGZ – Subgranular zone

SVZ – Subventricular zone

DCX - Doublecortin

NeuN - Neuronal specific nuclear protein

GFAP - Glial fibrillary acidic protein

DA - Dopamine

5HT - Serotonin

DAT - DA transporter

SERT - 5HT transporter

VMAT-2 - Vesicular monoamine transporter

GSH – Glutathione

CNS- Central nervous system

GLU - Glutamate

MAP2 - Microtubule-associated protein2

PARP - Poly (ADP-ribose) polymerase

DG - Dentate gyrus

CHAPTER 1: INTRODUCTION

1.1. Methamphetamine (METH)

1.1.1. History of METH Use

Methamphetamine (METH) is a methylated amphetamine (Chemical structures are presented in Figure 1.1) with psychostimulant properties. Amphetamine was synthesized in Germany in 1887 by Romanian chemist Lazăr Edeleanu, while METH was synthesized in 1893 by Japanese scientist Nagai Nagayoshi. Akira Ogata used iodine and red phosphorous synthesized crystallized METH in 1919. They provided the basis for production of the drug on a larger scale [1]. Amphetamine and METH were first used to help with respiratory problems and nasal congestion respectively. Thereafter, METH quickly became a popular medication during the 1940s and 1950s. During World War II, METH was used to help the soldiers stay alert. Abuse of the drug reached its peak in the 1960s. Following this, the Drug Abuse Control Amendments of 1965 and the Comprehensive Drug Abuse Prevention and Control Act of 1970 restricted the use of METH, and it was classified as a Schedule II drug [2]. In the 1980s, a crystalline form of METH that could be smoked, called “ice”, began to be imported from Asia to Hawaii [3]. This highly addictive form of METH quickly found its way to the U.S. West Coast and slowly began working its way east. By 1990, METH had replaced cocaine as the stimulant of choice among drug users in many areas of California [4]. With increasing numbers of large-scale manufacturers in Mexico and other parts of the world, METH continues to be a significant problem in the U.S. Today METH can only be prescribed for Attention Deficit Hyperactivity Disorder, extreme obesity, and narcolepsy. According to the Substance

Abuse and Mental Health Services Administration report, the number of patients treated for METH abuse increased by 50 percent in 2014 compared to 2009. The United Nations Office on Drugs and Crime reported that the amount of METH seized worldwide has increased by 158 percent during the last five years [5]. According to the World Drug Report 2015 (United Nations Office on Drugs and Crime 2015), North America continues to be one of the major consumers and producers of METH worldwide. This indicates that METH abuse should be considered a serious public health problem in the United States.

1.1.2. Properties of METH

METH comes in a variety of forms, such as a pure crystalline hydrochloride salt and formulated tablets. Routes of administration include intravenous injection, smoking, oral ingestion, and intranasal sniffing [6, 7]. Smoking is the most common route of administration. When smoked or injected, METH produces an intensely pleasurable initial rush that lasts only a few minutes, followed by an extended period of euphoria [8].

METH is a synthetic stimulant that affects the brain and central nervous system (CNS) [9]. It stimulates the release of dopamine (DA), serotonin (5-HT) and norepinephrine, and blocks their reuptake [10]. The presence of a large amount of these neurotransmitters in the synapses produces sensations of euphoria, feelings of invincibility, increased wakefulness, heightened sexual experiences, and hyperactivity that results from increased energy for extended periods of time. Deleterious short-term effects include rapid pulse, shallow breathing, hyperthermia, decreased appetite, increased respiration, confusion, irritability, chest pain, hypertension, convulsions, anxiety, aggressiveness, and symptoms of psychosis such as paranoia and hallucinations [11, 12]. This period is followed by mental and physical exhaustion, dizziness, reduced concentration, hunger,

decreased energy, and a desire for more METH [1]. Cognitive impairments and changes in the brain that result in symptoms similar to those of Parkinson's disease may occur [13]. Long-term use of METH is associated with neurotoxicity manifested as psychosis, anxiety, cognitive impairments, psychological dependence, and clinical depression that may lead to homicidal and suicidal ideation and action [8]. The medical use of METH is now confined to circumstances such as obesity, Attention Deficit Hyperactivity Disorder and narcolepsy [14].

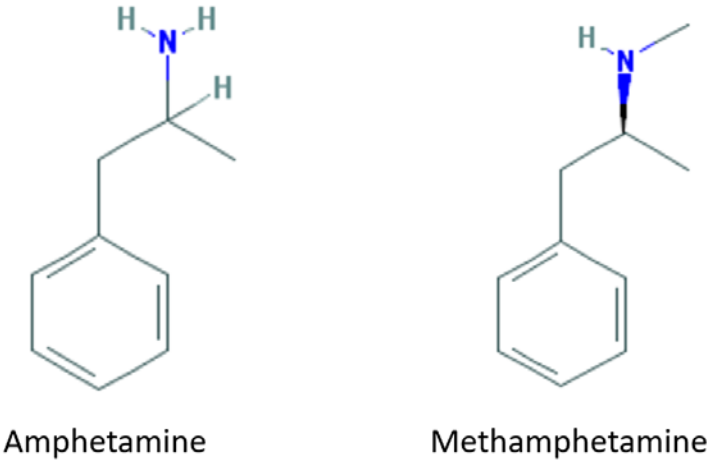

Figure 1.1. Chemical structures of amphetamine (left) and METH (right). (pubchem.ncbi.nlm.nih.gov).

1.1.3. Molecular Mechanism Underlying METH Abuse

Deep within the brain is a set of structures called the limbic system. It contains the brain's reward circuit, which controls and regulates our ability to feel pleasure [15]. Feeling pleasure is the primary motivation for humans to repeat drug-taking behavior. When the reward circuit is activated, each individual cell in the circuit produces chemical and electrical signals [16]. After METH administration, the drug quickly enters the brain. METH facilitates the release of the catecholamines DA, 5-HT, and noradrenaline from

nerve terminals in the brain, and inhibits their uptake. This leads to an increase in the synaptic concentration of these neurotransmitters and results in increased stimulation of postsynaptic receptors. To induce pleasurable effects, DA neurons release the neurotransmitter DA in the reward circuit. The released DA acts on DA receptors and actives a downstream signal. When a reward is encountered, the pre-synaptic cell releases a large amount of DA in a sudden burst. The excess of DA in the synaptic cleft is removed by DA transporters (DATs). Higher doses of METH can profoundly increase the release of DA from a neuron leading to high DA levels in the synapse where it becomes trapped since METH prevents the transporters from removing it [17]. The post-synaptic cell is activated to dangerously high levels because DA remains in the synapse, which causes powerful feelings of euphoria and makes METH incredibly addictive.

1.2. METH Neurotoxicity

METH can cause neurotoxicity. The Interagency Committee on Neurotoxicology defines neurotoxicity as permanent and reversible effects on the structure or function of the nervous system that can cause at least one of the following: loss of the neuronal components (e.g. synthesizing enzymes, receptors, transporters); a loss of the entire neuron and components therein (degeneration); histological signs of neuronal damage (silver staining, gliosis, swollen axons); and a persistent behavioral abnormality associated with the drug. This definition encompasses neuronal dysfunction in addition to degeneration, which is usually equalized with the term neurotoxicity. The established molecular mechanisms involved in mediating METH neurotoxicity include monoamine terminal (DAergic and 5HTergic) damage, mitochondrial dysfunction, hyperthermia, inflammation, excitotoxicity, and oxidative stress.

Hyperthermia occurs after the administration of high doses of METH [18, 19], and its occurrence is important for the development of METH neurotoxicity in DA and 5-HT terminals. For instance, in mice, multiple injections of high-dose METH at room temperature produced a significant depletion of DA in the striatum; however, equivalent doses of METH administered in a cold environment blocked striatal DA and 5-HT depletions [20]. Hyperthermia by itself does not decrease striatal DA levels in rodents [21]. Hyperthermia might interact with other known mediators of METH neurotoxicity, such as increased glutamate (GLU) neurotransmission and oxidative stress [22]. For example, inhibition of METH-induced hyperthermia decreases the formation of reactive oxygen species (ROS) in the striatum that, in turn, attenuates the damage to DA terminals [23].

1.2.1. METH Effects on Catecholaminergic Neuronal Terminals

METH treatment can cause acute increases in both DA and 5-HT release, because of the action of the drug on DAT and 5-HT transporters (SERT). METH is known to be a substrate for both transporters and is transported into the axon terminal [24, 25]. After its intracellular transport (transporter- or diffusion-mediated) into the terminal, METH disrupts the storage vesicle proton gradient and causes the release of DA and 5-HT from vesicular compartments into the cytoplasm [26]. Cytoplasmic monoamine concentrations and DA release can be affected by METH via alteration of the function of the vesicular monoamine transporter (VMAT-2) [27, 28]. The directionality of the DA and 5-HT transporters can be reversed by increasing cytoplasmic DA and 5-HT levels, and causes significant, action potential-independent neurotransmitter efflux [29]. Short-term decreases in neurotransmitter reuptake also contribute to increases in extracellular DA

levels [30]. In addition, METH causes acute increases in striatal GLU levels via D1 receptor-mediated disinhibition of corticostriatal GLU release [31].

Binge METH administration is an established drug regimen causing neurotoxicity that includes degeneration of DAergic and 5-HTergic terminals in the striatum, hippocampus, and prefrontal cortex of experimental animals [32, 33]. Acute effects of METH include persistent DA and 5-HT terminal damage, manifested by long-term decreases in DAergic and 5-HTergic markers, in the striatum, hippocampus, and prefrontal cortex [32, 33]. The damage associated with METH has been shown to persist for at least two years in rodents and non-human primates [34, 35]. The expression of certain neurochemical markers, such as tryptophan hydroxylase and tyrosine hydroxylase, which are the rate-limiting enzymes for 5-HT and DA respectively, decreases after METH treatment. There is also a decrease in DAT and SERT expression [33, 36]. Excepting tissue content and neurotransmitter proteins, histological signs of neuronal damage have been reported which include the presence of swollen and distorted nerve terminals [37, 38]. Chronic administration of high METH doses also leads to neurotoxicity. Long-term METH abuse, which can damage DA and 5-HT nerve terminals, is associated with deficits in neuropsychological test performance, and it has been estimated that 40% of METH users display abnormalities on neuropsychiatric tests [39]. Chronic METH exposure converges to produce neuronal damage and inflammation [20]. A persistent reduction in most DA markers [13, 40] and SERT [41] has also been observed in human chronic METH users.

1.2.2. METH and Neuronal Apoptosis

There is some supporting evidence indicating that METH may induce apoptosis or even cell death in some neuronal populations, in addition to damaging DA and 5-HT

terminals [42]. Apoptosis is a cell suicide program that is initiated after exposure to cytotoxic stressors, including UV, IR irradiation, chemotherapeutic drugs, and hypoxia. The marker for apoptotic cell death, Terminal deoxynucleotidyl transferase dUTP nick end labeling (TUNEL), increases in the striatum after exposure to METH [42, 43]. Importantly, METH administration affects brain functions, such as long-term memory, integrative functions, and attention [44], conditions which reflect hippocampal degeneration. The hippocampus is an important area in the temporal lobe of the brain. It plays a role in cognitive function including short-term memory, motivation, and emotional responses. Hippocampal degeneration has been observed in animals after exposure to high-dose METH [45]. METH-induced cell death was reported in the cortex, hippocampus, and hippocampal remnants [46]. Some papers have demonstrated cell death of calbindin-containing GABA interneurons within the hippocampus in animal models [45, 47]. In the striatum, METH causes apoptosis in neurons post-synaptic to striatal monoaminergic terminals [46, 48, 49]. The apoptotic cells have been identified in subpopulations of GABA-interneurons, such al parvalbumin-containing striatal GABA interneurons [44]. METH-induced apoptosis in neuronal cell bodies is associated with mitochondrial damage and endoplasmic reticulum stress [42]. At the same time, METH causes DNA damage and alterations in the expression of Bcl-2 related genes, which may contribute to cell death in GABA interneurons [50]. METH can also induce apoptosis through increases in caspase-3 activity and the Fas/FasL cell death pathway [51].

1.2.3. METH and Inflammatory Response

METH has been reported to trigger inflammatory responses in areas where DA and 5-HT terminals are damaged. METH elicits microglial activation in rat and mouse striati

[52, 53], rat cortices (including somatosensory and frontal cortices) [45, 54] and hippocampi [55]. Moreover, METH can trigger the release of some pro-inflammatory cytokines, which can lead to glial dysfunction as well as neuronal death [55, 56]. METH also induces reactive gliosis supported by the observation of increased glial fibrillary acidic protein (GFAP) immunoreactivity in the striatum [57], hippocampus, and indusium griseum [58]. Reactive gliosis is considered to be a universal reaction of injury in the CNS and is used as a specific marker of neuronal damage.

METH-induced release of GLU also contributes to the activation of inflammatory mediators which enhance the METH toxicity to monoaminergic as well as non-monoaminergic neurons [20]. For instance, GLU receptor activation is known to stimulate microglial activation whereas GLU antagonism suppresses the appearance of microglial activation [59]. Furthermore, during METH exposure, microglial activation and increases in GLU are seen in the striatum, prefrontal cortex, and hippocampus [60].

1.2.4. METH and Oxidative Stress

Reactive oxygen species are produced following METH exposure through numerous mechanisms. When cytoplasmic DA increases following exposure to pharmacologically relevant METH levels [61], DA-dependent oxidative stress has been observed due to DA autoxidation [62]. Dopamine can also cause oxidative stress via its metabolism by monoamine oxidase (MAO) which can induce the generation of superoxide and hydrogen peroxide free radicals [63]. Hydrogen peroxide can react with iron via the Fenton reaction and generate hydroxyl radicals, which are highly reactive and can result in damage by causing DNA mutations, lipid peroxidation, and modification of certain amino acids [64]. Damage to lipids and proteins causes DAergic terminal loss. Moreover, METH

exposure can cause oxidative stress because it can increase nitric oxide synthase activity and consequently increase the reactive nitrogen species [65]. Impairment of mitochondrial function has also been linked to pathways generating ROS, which can lead to an oxidized environment and decreased ATP production [66]. Oxidative stress can be further enhanced by dysfunction of antioxidant enzymes [67]. Enzymatic antioxidant defenses (e.g. catalase, superoxide peroxidases, and enzymes of the glutathione antioxidant system) serve to counterbalance the effect of oxidants such as hydrogen peroxide, hydroxyl radical, and superoxide radical. The activity of glutathione peroxidase (GPx) depends on the availability of reduced glutathione (GSH), which is the most important non-enzymatic antioxidant [68]. Antioxidant treatments have been shown to be neuroprotective against the damage produced by METH. This finding substantiates the significant contribution of oxidative stress to the neurotoxicity of amphetamines [69].

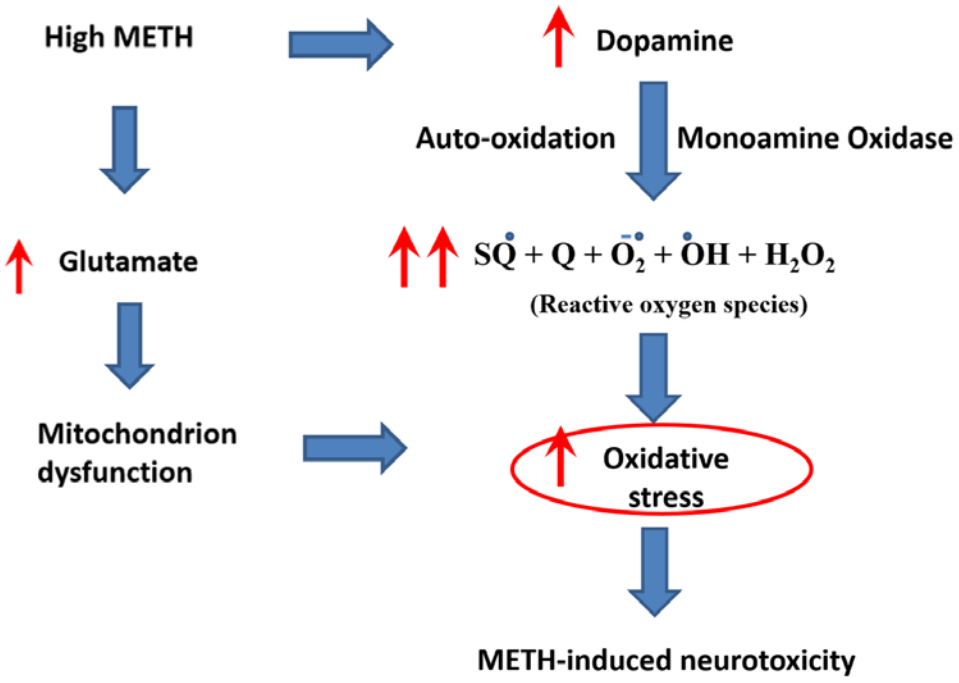

Figure 1.2. Oxidative stress in METH toxicity. As high levels of METH enter the DAergic terminal, DA is released from storage vesicles, and triggers the generation of many reactive oxygen species (ROS). High-dose METH also enhances the release of glutamate in the striatum, leading to excitotoxicity. The generation of ROS and excitotoxicity can increase the oxidative stress, which enhances the METH-induced neurotoxicity.

1.2.4. Markers for Apoptosis and Oxidative Stress

Apoptosis is a programmed cell death. Caspases are the central mediators of this process. In mammals, caspases involved in apoptotic responses are classified into two groups according to their function and structure. The first group is termed initiator caspases (caspase-2, 8, 9, 10) that contain N-terminal adapter domains that allow for auto-cleavage and activation of downstream caspases. The second group is termed effector or executioner caspases (caspase-3, 6, 7) that lack of N-terminal adapter domains and are cleaved and activated by initiator caspases [70]. Caspases-3 and 7 are critical mediators of mitochondrial dysfunction-mediated apoptosis. For example, they can amplify the initial death signal by promoting cytochrome c release [71]. Under intrinsic stress, cleaved caspase-3 is produced via cleavage of caspase-9, which is considered to be the marker of middle stage apoptosis.

Poly (ADP-ribose) polymerase (PARP), a nuclear enzyme, has a particularly well-researched role in base excision repair [72]. In addition to being involved in DNA repair, PARP is also directly involved in both apoptosis and necrosis [73, 74]. Caspase-3 can cleave PARP, and thus inactivate and inhibit PARP's DNA-repairing abilities. Therefore, cleaved PARP may be considered a marker of late apoptosis [75].

1.2.5. Antioxidant Mechanisms in the Brain

The brain has a high rate of aerobic metabolism, therefore it is one of the major organs generating large amounts of ROS and is especially susceptible to oxidative stress. GSH plays a critical role as an antioxidant in the brain due to its capability to scavenged multiple ROS [76]. GSH levels can increase or decrease after METH administration, depending on the severity of METH-induced oxidative stress [77-79]. Thus, changes in levels of GSH could be a sign of oxidative stress.

1.2.6. METH Neurotoxicity in Experimental Animals vs. Humans

As mentioned above, METH is a neurotoxic drug that causes deficits and alterations in central DAergic pathways. Repeated administration of METH in rodents has been shown to cause neurodegeneration of DAergic axon terminals in the striatum. The signs of METH-induced neurodegeneration of DAergic axon terminals include reduced levels of DAergic markers, for example DAT, VMAT2, and TH as well as the levels of DA and its metabolites including: 3,4-dihydroxyphenylacetic acid (DOPAC), 3-methoxytyramine (3-MT) and homovanillic acid (HVA). These effects occur primarily in the striatum but are also seen in the cortex, thalamus, hypothalamus, and hippocampus [52, 80]. METH induces neurotoxicity in a dose-dependent manner [81]. METH has high popularity due to its wide availability, relatively low cost, and long duration of psychoactive effects. The neurotoxic effects of METH in humans are similar to those observed in experimental animals. For example, when administrated at high doses, METH can cause selective decreases in DAergic and 5-HTergic markers in both experimental animals and humans [82]. Neuroimaging studies of METH abusers have revealed reduction in striatal DAT levels that are associated with motor slowing and memory impairment [13, 83]. There is also a report demonstrating that METH alters dentate gyrus (DG) stem cell properties by delaying

the cell cycle and decreasing self-renewal capacities. DG neurogenesis impairment could be the mechanism of cognitive deficits verified in METH consumers [84]. These effects could be manifestations of METH-induced degeneration, however, growing evidence suggests that neuronal degeneration may not be a part of METH neurotoxicity in human METH users [85].

1.3. Transposable Elements and Long Interspersed Element 1

1.3.1. METH and Epigenetic Changes

Recently, epigenetics change has attracted much attention as a new and promising research area in METH abuse [86]. Several studies have reported that acute and chronic administration of METH can significantly influence the expression of many genes in the nucleus accumbens and dorsal striatum [87]. Recent reports show that the changes in histone modifications are related to the expression of genes coding for a variety of proteins that occur after self-administration of high-dose METH [87]. Moreover, decreased expression of several histone deacetylases (HDACs) occurs in the striatum after neurotoxic binge METH [88]. In the substantia nigra, high-dose METH injection over four days can decrease DNA methylation within the promoter region of alpha-synuclein [89].

1.3.2. Transposable Elements and LINE-1

Activation of transposable elements (TEs) is considered to be an epigenetic change [90]. Transposable elements are common and naturally occurring sources of genetic variation known to play diverse roles in genome evolution [91]. However, there are very few studies that have investigated the effects of METH on TEs *in vivo*. Among all TEs, long interspersed element 1 (LINE-1) is the most abundant and active endogenous

retroelement, accounting for 17% of the human genome [92, 93]. There are thousands of copies of LINE-1 in a single human cell, and most of them are silenced under normal physiological conditions. In the human genome, 80–100 copies of LINE-1 are capable of retrotransposition [94], and 10% of these are highly active via the *copy and paste* mechanism that involves an RNA intermediate and reverse transcriptase activity [95] (Figure 1.4). A complete cycle of LINE-1 retrotransposition can be associated with DNA inversions, duplications, or insertions [96]. LINE-1 is 6 kb in length and consists of a promoter, two open reading frames (ORF-1 and ORF-2), and a poly(A) tail [93, 97] (Figure1.4). ORF-1 is a basic protein with a nucleic acid chaperone and RNA binding activity. It is present within cytoplasmic ribonucleoprotein complexes or stress granules in the cytoplasm [98, 99]. ORF-2 has dual functions of endonuclease [100] and reverse transcriptase [101]. ORF-1 and ORF-2 mediate LINE-1 retrotransposition, which proceeds through three steps: transcription, reverse transcription, and insertion of the new synthesized DNA into the host genome via target site-primed reverse transcription [93, 102]. According to the literature, LINE-1 can be expressed and undergo retrotransposition at a high frequency in the mammalian nervous system [103, 104]. Furthermore, deregulation of LINE-1 retrotransposition is involved in some neurological diseases such as Rett syndrome and ataxia telangiectasia [104]. Since LINE-1 retrotransposition can change cellular properties by causing gene deletions [105], DNA damage [102], apoptosis [106], and immune response [107], deregulation of LINE-1 in somatic cells is likely to occur as either a cause or a consequence of a disease. Our lab has shown that binge METH increases ORF-2 protein levels in the neurogenic zones of rat brains [86]. In neuronal cell lines, METH has been shown to trigger retrotransposition of LINE-1 [108].

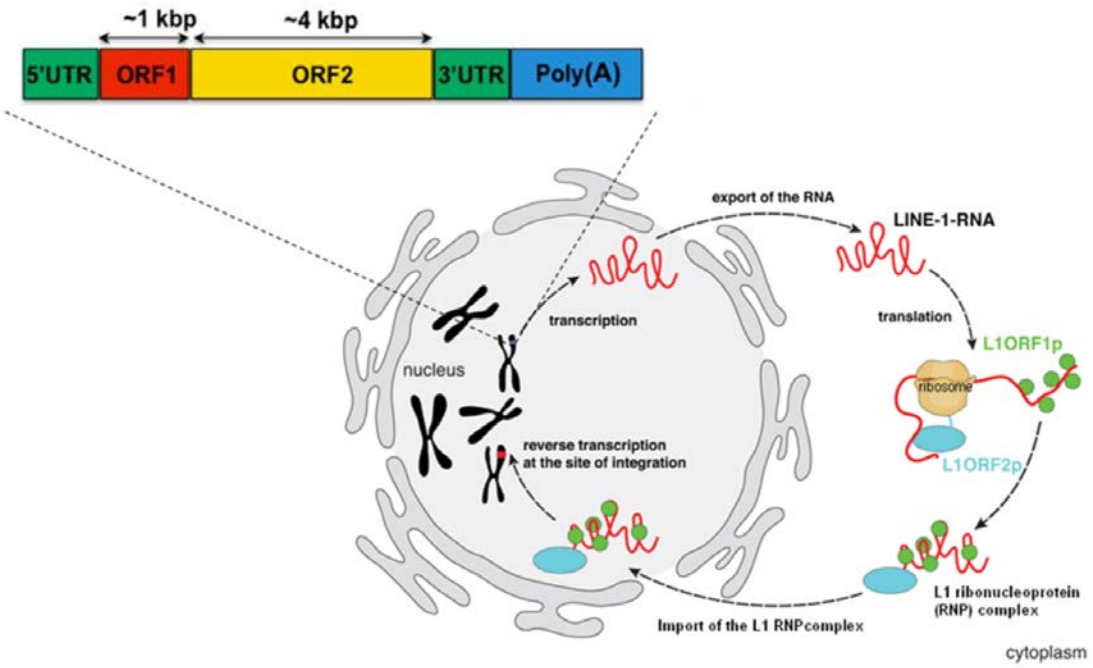

Figure 1.3. LINE-1 structure and activation. LINE-1 is 6 kb in length and consists of a promoter, two open reading frames (ORF-1 and ORF-2) and a poly(A) tail. ORF-1 and ORF-2 mediate LINE-1 retrotransposition, which proceeds through 3 steps: transcription, reverse transcription, and insertion of the new synthesized DNA into the host genome via target site-primed reverse transcription.

1.4. Neurogenic Zones and Neurogenesis

1.4.1. Neurogenesis

The dogma that the adult mammalian brain does not generate new neurons has been overturned [109]. It has been reported that thousands of new neurons are generated every day in an adult mammalian brain [110]. Adult neurogenesis is a process of generating functional neural cell types from neural stem cells and progenitor cells; it is important for the maintenance of brain integrity and optimal function [111]. This process occurs in two separate areas of the adult mammalian brain, the subgranular zone (SGZ) and the subventricular zone (SVZ) [111-113]. In the SGZ of the DG in the hippocampus, adult neural stem cells undergo proliferation, fate specification, maturation, migration, and

eventual integration into the pre-existing neural circuitry within the hippocampus [114, 115]. Principal DG cells are the only neuronal subtype that is generated, and newly generated neurons have distinct properties that enable them to contribute to specialized functions in learning and memory [116]. Subventricular zone neurogenesis is related to olfactory bulb formation [117] and may represent a potential source of cells used to repair damaged brain tissue [118]. In the SVZ of the lateral ventricle, adult neural stem cells give rise to glia and neuroblasts [117]. These neuroblasts migrate over a long distance to the olfactory bulb and differentiate into local interneurons that have various functions in olfaction.

The SGZ is located in the hippocampus between the hilus and the granule cell layer of the DG (Figure 1.5). Previous studies have shown that after newborn neurons mature and migrate from the granule layer in the adult DG, they form axonal projections and reach the CA3 [119]. There are main four types of cells in the SGZ. Type-1 cells (radial-glia-like stem cells) have astrocyte characteristics and they express GFAP and nestin [120, 121]. Type-1 cells divide asymmetrically. They can either proliferate to other Type-1 cells to maintain their own population or differentiate into the intermediate cells, called type-2 cells (neural progenitor cells, 2a and 2b). Type-2 cells generate the migratory neuroblasts known as type-3 cells. Type-3 cells migrate into the granule cell layer and differentiate into granule neurons. Type-4 cells, after having ceased mitosis, extend axons toward the CA3, leading to the development of mature neurons which are positive for neuronal specific nuclear protein (NeuN) and calbindin. Type-4 cells integrate with the mossy fiber pathway [122].

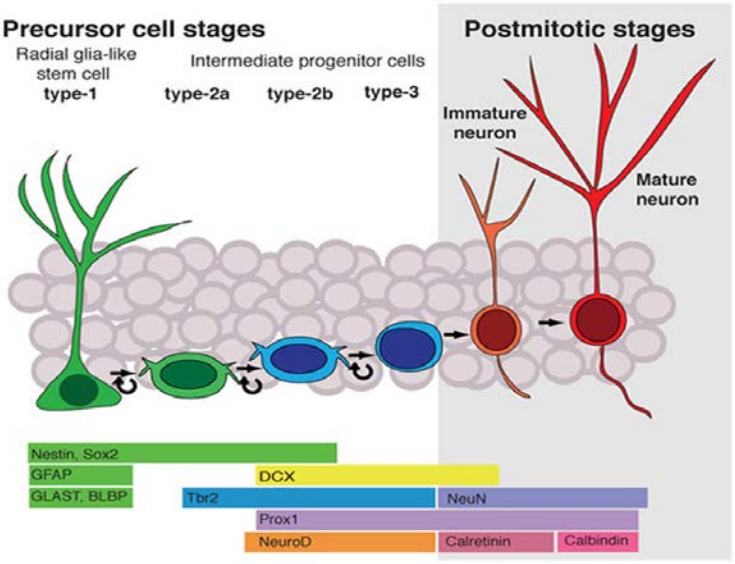

Figure 1.4. Neurogenesis in the subgranular zone (SGZ). Top panel: type-1 cells generate type-2 cells that, in turn, generate type-3 cells; type-3 cells generate immature neurons that finally become mature neurons. Bottom panel: a sequence of cell types involved in neuronal lineage and specific markers allowing cell identification are presented.

The SVZ is a second site of neurogenesis in the adult brain. New neurons formed in this region constantly migrate toward the olfactory bulb to replace interneurons [123]. In the olfactory bulb of adult rats, approximately 80,000 new granular neurons are formed each day from the SVZ progenitors [124]. The SVZ is formed by three main cell types: type A, B, and C cells. The type-A cells are migratory neuroblasts. Approximately 33% of the SVZ cells are type-A cells. They express doublecortin (DCX) and polysialylated neuronal cell adhesion molecule (PSA-NCAM). They migrate through the rostral migratory stream (RMS) to the olfactory bulb where they differentiate into granular and glomerular neurons. In the SVZ, about 23% of cells are type-B cells, which give rise to type-C cells. Type-B cells are slow proliferating multipotent cells expressing GFAP. They have the characteristics of astrocytes and can be classified as B1 and B2 cells. B1 cells are in contact with the lateral ventricle lumen and have a small apical surface, a single basal

body, and a single short primary cilium. The Type-C cells are transit-amplifying immature precursor cells that account for about 11% of the SVZ cells. They produce type-A cells and express the transcription factor distal-less homeobox 2 (Dlx2) [124] and nestin [125].

1.4.2. Markers for Neurogenesis in the Neurogenic Zones

In this study, we used specific markers to differentiate diverse cell types. The specific markers include: (a) Proliferating cells: Ki-67 is a nuclear protein expressed in dividing cells for the entire duration of their mitotic activity, the expression of which is neither linked to DNA repair nor to apoptotic processes. Therefore, it is used as a reliable marker for proliferating cells) [126, 127]; (b) Immature neurons: DCX can encode a microtubule-associated protein expressed in migrating neuroblasts therefore it can serve as a marker of immature neurons [128]; (c) Mature neurons: NeuN, a neuronal specific nuclear protein, is the most frequently used specific marker for mature neurons [129]. Another common marker for mature neurons is microtubule-associated protein (MAP-2). (d) Astrocytes: GFAP is a common marker for astrocytes [125].

The cell composition of the SGZ and SVZ and their markers are presented in Figure 1.5 and Figure 1.6, respectively.

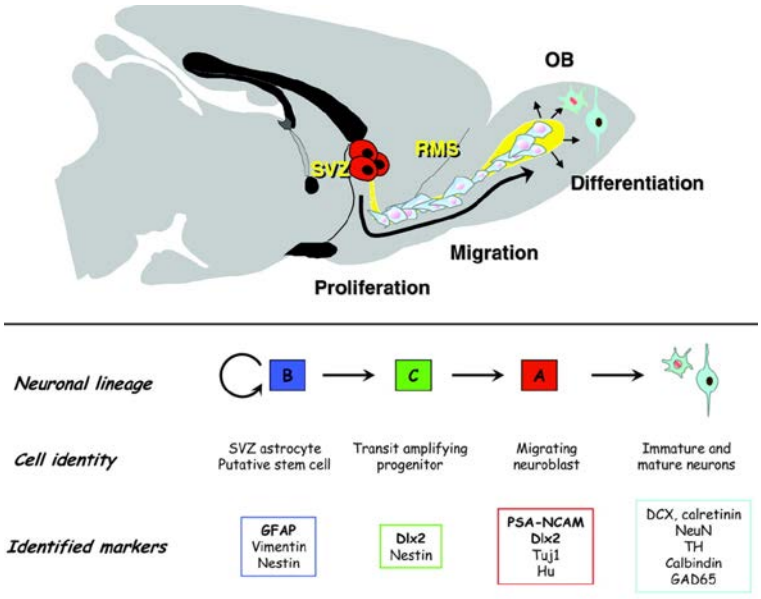

Figure 1.5. Neurogenesis in the subventricular zone (SVZ). Top panel: a sagittal view of a rodent brain showing the sites of neurogenesis in the SVZ/olfactory (OB) system. Cells that proliferate in the SVZ migrate along the rostral migratory stream (RMS) to reach the OB, where they migrate radially and undergo terminal differentiation. Bottom panel: a sequence of cell types involved in neuronal lineage and specific markers allowing cell identification are presented. Markers appearing in bold are specific to each stage.

1.4.3. METH effects in the neurogenic zones

METH abuse in humans severely damages the hippocampus, for example by reducing hippocampal volume and producing hippocampal-dependent memory deficits [130]. As stated previously, adult neurogenesis has been demonstrated in the hippocampal SGZ [131]. Recently, it has been shown that a number of external factors, such as drug abuse can regulate the birth, survival, and fate of newly-generated SGZ progenitors [132]. METH has been reported to dysregulate neurogenesis and induce apoptosis in the hippocampus and often leads to the death of pyramidal neurons and granular cells [133, 134]. Intermittent (occasional access) and daily (limited and extended access) self-administration of METH can have an impact on different aspects of hippocampal neurogenesis [134]. According to a study aiming to clarify the effect of METH on SVZ

stem/progenitor cell dynamics and neurogenesis, high dosages of METH triggered cell death both by necrosis and apoptosis, and inhibited the proliferation of progenitor cells in the SVZ. Furthermore, another study reported that, at non-toxic concentrations, METH treatment decreased neuronal differentiation and maturation [135].

1.5. Rationale, Objective, and Hypotheses

In our previous study, we found that binge METH increased expression of ORF-2 in the neurogenic zones in rat brains and that some of the ORF-2-positive neurons were also positive for DCX. But we did not identify all cell types that showed increased ORF-2 levels after METH administration. Additionally, we did not determine the potential functions of increased ORF-2. The major objective of the current study is to differentiate the cell populations expressing ORF-2 and to discover whether upregulation of ORF-2 is associated with oxidative stress and/or apoptosis in the neurogenic zones after exposure to binge METH.

Our previous study showed that METH can activate LINE-1 *in vivo*, and trigger retrotransposition of LINE-1 *in vitro* [108]. Moreover, TEs undergo retrotransposition mostly in proliferating cells [135], LINE-1 activation can lead to DNA breakage suggesting that LINE-1 may cause apoptosis. It has been reported that binge METH induces apoptosis in the neurogenic zones. Cytoplasmic and extracellular DA levels increase dramatically after METH exposure [61], which lead to increased ROS production and oxidative stress [65]. Furthermore, METH-induced increases in GLU release cause mitochondrial dysfunction thus further potentiating oxidative stress [136]. On the base of these knowledges, we hypothesized that neurotoxic binge METH would activate LINE-1 in

proliferating cells in the neurogenic zones and the METH-induced increases in LINE-1 activity would be associated with apoptosis and oxidative stress.

CHAPTER 2: MATERIALS AND METHODS

2.1. Animals

Adult male Sprague-Dawley rats (weighing 250–300g) were accommodated in a pair-housed, humidity-controlled room and temperature-controlled (20–22 °C). Food and water were provided. We allowed all the rats to acclimatize for seven days before we start the research. Our animal procedures have been approved by the Institutional Animal Care and Use Committee (IACUC) at Wayne State University. All the animal procedures were conducted between 7:00 A.M. and 7:00 P.M. in strict accordance with the National Institutes of Health (NIH) Guide for the Care and Use of Laboratory. The description of animal procedures meets the ARRIVE recommended guidelines described by The National Centre for the Replacement, Refinement, and Reduction of Animals in Research.

2.2 Drug Treatment

(+)-METH hydrochloride (METH, 10 mg/kg free base) (Sigma-Aldrich, St. Louis, MO) or saline (1 mL/kg) was administered to the rats every 2 h in four successive intraperitoneal (i.p.) injections. We measured the core body temperatures of the rats before the starting of saline/ METH administration and the core body temperatures at 1 hour after each injection and sacrifice the rats 24 hours after the last injection of saline/ METH.

2.3. Tissue Collection and Storage

We removed the brain from rats and washed with ice-cold phosphate-buffered saline (PBS). The brains were fixed in 4% paraformaldehyde for 24 h at 4°C. After fixation, the brains were incubated in 20% and then in 30% glycerol in PBS (24 h in each solution at 4 °C). Subsequently, the brains were snap-frozen and stored at − 80 °C until assayed.

2.4. Tissue Immunohistochemistry

We checked the protein level via immunofluorescence technique. We used the tissue sections (40 μm) from the SVZ (1.16 to 0.28 according to Bregma) and the SGZ (−3.14 to –4.66 according to Bregma). We permeabilized the tissue sections with PBS + 0.1% triton and did antigen retrieval using 1× citrate buffer for 30-45 min at 90°C. We blocked the tissue at room temperature using blocking buffer (PBS pH 7.4, 0.1% Triton X-100, and 5% bovine serum albumin (BSA)) for 1 hours after cooled the sections to room temperature. The sections were then incubated overnight at 4°C with a chicken anti-ORF-2 antibody (1:200, Rockland Immunochemicals Inc., Limerick, PA) and a cell type marker antibody ,a rabbit anti-GFAP (1:200, Cell Signaling, Danvers, MA), rabbit anti-NeuN (1:400, Cell Signaling), rabbit anti-Ki-67 (1:100, Abcam, Cambridge, MA) or rabbit anti-doublecortin (1:100, Abcam) antibody or an apoptosis marker antibody (a rabbit anti-cleaved PARP (1:200, Abcam) or rabbit anti-cleaved caspase-3 (1:400, Cell Signaling) antibody. In the last experiment, the sections were double-labeled with the anti-ORF-2 antibody and mouse anti-GSH (1:200, Abcam) antibody. The next day, We washed the section with washing buffer (PBS pH 7.4, 0.1% Triton X-100, and 5% bovine serum albumin (BSA)) for three times (5 min per washing) and incubated the sections with secondary antibody, anti-chicken Alexa-488 (1:1000) and anti-rabbit Alexa-594 (1:1000) (Life Technologies,

Carlsbad, CA) for 2 hours in room temperature. We stained the nuclei using DRAQ5 (Life Technologies). Lastly, we mounted the sections on slides using Flouromount mounting medium (Sigma-Aldrich) and cover the slips. We captured the images via Leica TCS SPE-II confocal microscope under the 63 × oil objective. These images were then analyzed using Leica co-localization analysis software. The ORF-2 immunofluorescence was measured by Image J and averaged. Mean of the averages was then calculated for each rat.

2.5. Cell Culture

PC12 cells (a rat adrenal gland pheochromocytoma cell line) were cultured on sterilized coverslips (Warner Instrument, Hamden, CT) in the HyClone RPMI-1640 medium (GE Healthcare Life Sciences) containing 5% fetal bovine serum (FBS) and 10% horse serum. The coverslips were placed in wells of a 24-well plate; each well was seeded with approximately 50,000 cells.

2.6. Cultured Cells Immunocytochemistry

The next day, the cells were treated with 2mM glutamic acid for 1h, 2h, 3h, 4h, 5h, 6h, 12h or 24h at room temperature. Next, the cells were fixed in 4% paraformaldehyde for 20 min and then permeablized using 0.1% Triton X-100 in PBS for 1h at room temperature. Subsequently, the cells were blocked in blocking buffer (0.1% Triton X-100, and 1% BSA in PBS) for 1h at room temperature and incubated overnight at 4°C with the chicken anti-ORF-2 antibody (1:1000, Rockland Immunochemicals Inc.) or rabbit anti-cleaved caspase-3 antibody (1:400, Cell Signaling). The next day, We washed the section with washing buffer (PBS pH 7.4, 0.1% Triton X-100, and 5% bovine serum albumin (BSA)) for three times (5 min per washing) and incubated the sections with secondary antibody, anti-

chicken Alexa-488 (1:1000) and anti-rabbit Alexa-594 (1:1000) (Life Technologies, Carlsbad, CA) for 2 hours in room temperature. We stained the nuclei using DRAQ5 (Life Technologies). Lastly, we mounted the sections on slides using Flouromount mounting medium (Sigma-Aldrich) and cover the slips.

2.7. Statistical Analysis

We analyzed the data using two-way ANOVA (factors: regions and treatment) followed by Bonferroni *post hoc* test. Two-way repeated measures (RM) ANOVA was used for analysis of temperature data. Correlations between measured parameters were performed using Pearson's correlation analysis. Significance was set at $p < 0.05$ (95% confidence interval) and we further analyzed data using GraphPad Prism program (GraphPad Software Inc., San Diego, CA, USA).

Chapter 3 RESULTS

3.1. Binge METH Induces Hyperthermia

In experimental rodents, high doses of METH are known to cause hyperthermia, which is one of the factors that mediate the neurotoxicity of the drug. An increased core body temperature can promote the METH induced neuro-toxicity, while a lower body temperature reduces the METH-induced toxicity [18, 20]. We measured the core body temperatures of the rats before the starting of saline/ METH administration (baseline temperatures) and the core body temperatures at 1 hour after each injection. As shown in Figure 3.1, a significant increase in body temperature was observed in METH-treated animals (**p<0.005, n=6, by two-way ANOVA followed by Bonferroni post hoc test).

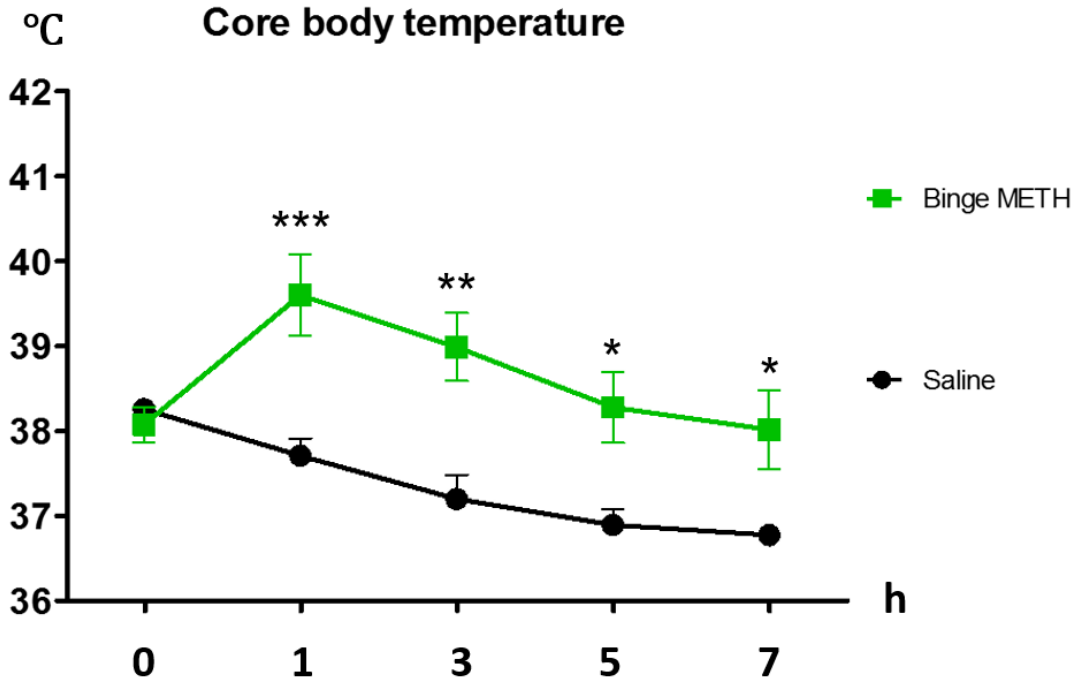

Figure 3.1. Hyperthermia during binge METH treatment. We observed a significant increase ($F(4,50) = 4.97$, $^{**}p < 0.005$, n=6, by two-way ANOVA) in rat core body temperature. The two-way ANOVA showed a significant increase in core body temperature at 1 h ($^{***}p < 0.001$, n = 6), 3 h ($^{**}p < 0.005$, n = 6), 5 h and 7 h ($^{*}p < 0.05$, n = 6) after binge METH. Abbreviations: h, hour(s); METH, methamphetamine.

3.2. Binge METH Increases ORF-2 Protein Levels in Neurogenic Zones

A previous study conducted in our lab showed that ORF-2 increased in the neurogenic zones at 24 hours after binge METH [3]. Therefore, we first examined rats' brains for ORF-2 protein immunoreactivity in the SGZ and SVZ (average of 3 locations outlined in Fig. 3.2). Similar to previous results, low ORF-2 protein immunoreactivity was observed in neurogenic zones in the saline-treated rats, while significantly higher ORF-2 protein immunoreactivity was detected in both the SGZ and SVZ in METH-treated rats (Fig. 3.3) (+75.5%, $^{***}p< 0.001$ and +125%, $^{***}p< 0.001$, respectively, n=6, by two-way ANOVA followed by Bonferroni post hoc test), thus confirming the results of our previous study.

Figure 3.2. A schematic illustration of the subgranular zone (SGZ) and subventricular zone (SVZ). In the adult rodent brain, (a) the SGZ lies below the granular cell layer of the DG whereas (b) the SVZ lies between the lateral ventricle and the striatum, as shown by red markers. Representative images were taken from these 3 regions of the SGZ (a) and the SVZ (b) per condition (saline vs. METH).

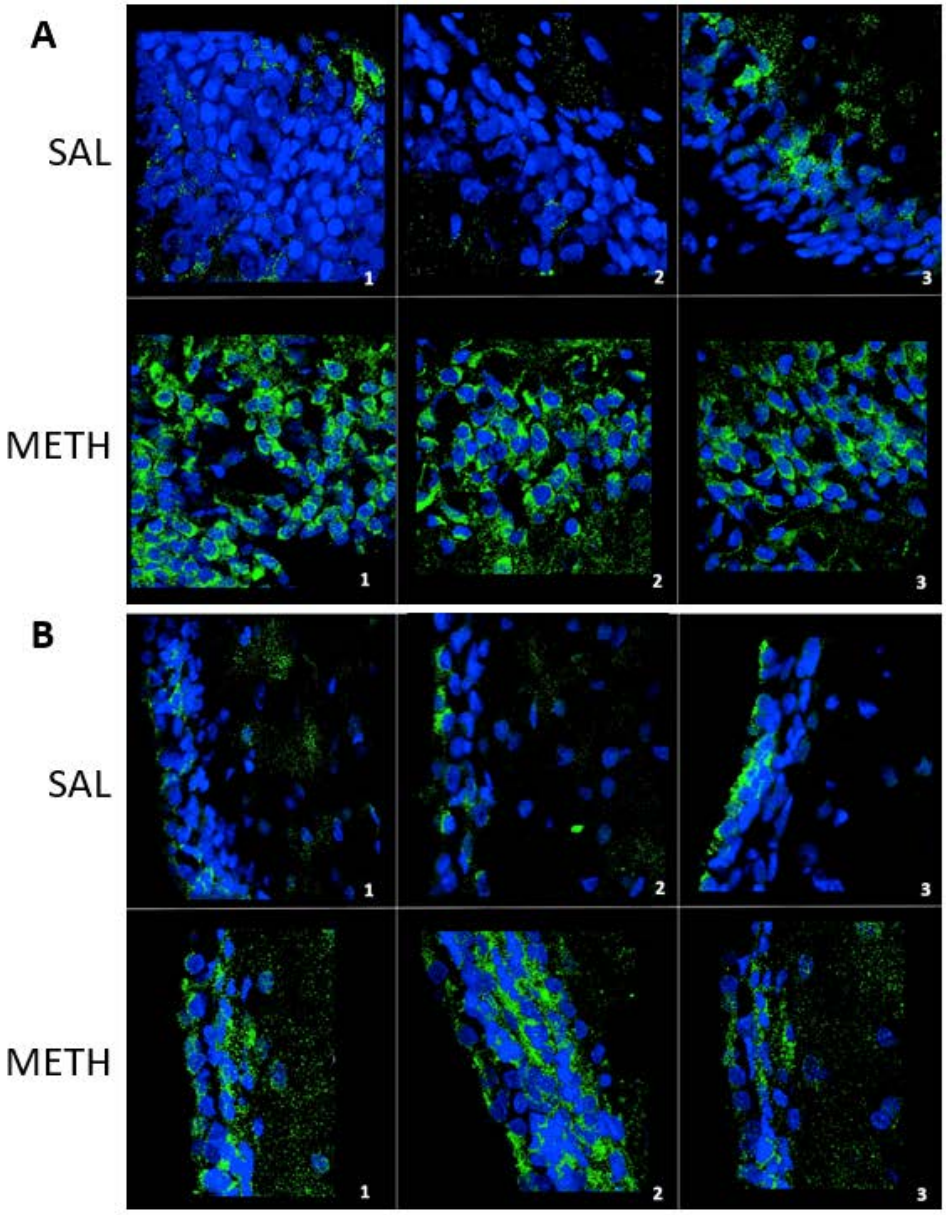
A
SAL
METH
1
2
3
B
SAL
METH
1
2
3

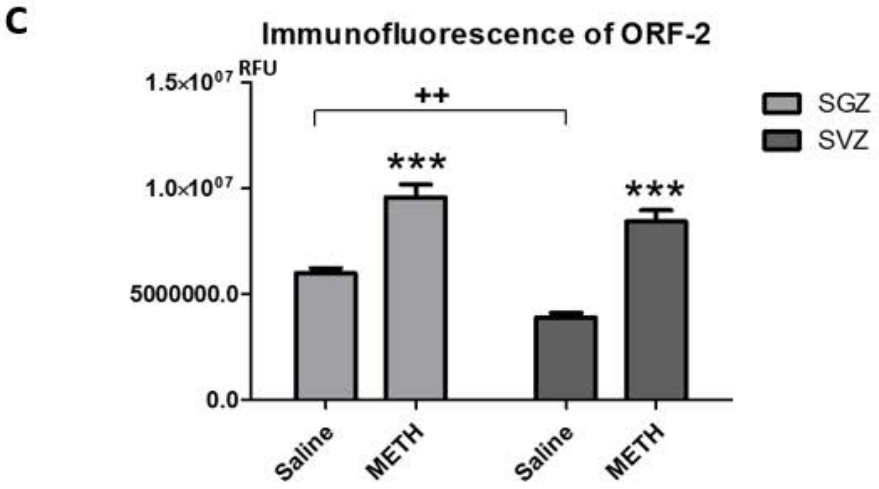
C
Immunofluorescence of ORF-2
RFU
1.5×10^07
1.0×10^07
5000000.0
0.0
++
***
***
SGZ
SVZ
Saline
METH
Saline
METH

Figure 3.3. Binge METH increases immunoreactivity of ORF-2 in the neurogenic zones. Shown are representative images taken from 3 regions of the SGZ (A) and the SVZ (B). The two-way ANOVA showed significant effect in ORF-2 signal (green) of treatment ($F(1,20) = 13.7$, $^{**}p < 0.005$, n=6) & region ($F(1,20) = 128$, $^{***}p < 0.001$, n=6). Bonferroni post-tests revealed a significant increase in ORF-2 in both SGZ and SVZ between treatment (+75.5%, $^{***}p < 0.001$, and +125%, $^{***}p < 0.001$, n=6). Bonferroni post-tests revealed significant decrease in ORF-2 in the saline-treated group but not the METH-treated group between regions (-31.9%, $^{***}p < 0.001$, and -9.02%, $^{***}p < 0.001$, respectively, n=6). The data are summarized in (C). Nuclei are depicted in blue. Abbreviations: METH, methamphetamine; SAL, saline; ORF-2; open reading frame 2; SGZ, subgranular zone; SVZ, subventricular zone.

3.3. Identification of Cell Types Expressing Activated LINE-1 in the Neurogenic Zones after Binge METH

3.3.1. Intermediate progenitor cells and neuronal cells

The intermediate progenitor cells include types 2a, 2b, and 3 cells within the SGZ and types A and C cells in the SVZ. The cells that proliferate rapidly within the SGZ are type 2 and some type 3 cells, whereas the cells that proliferate within the SVZ are type A and C cells. In the SGZ, type 2b and type 3 progenitor cells, as well as postmitotic immature neurons express DCX protein (Fig.3.6.A). Immature and mature neurons, but not the intermediate progenitor cells, can be identified by NeuN protein in this zone (Fig.3.7.A). In the SVZ, neuroblasts express DCX (Fig.3.6.B) while mature neurons express NeuN (Fig.3.7.B). MAP2, as a marker of neuronal cells, can be used for cytoskeleton staining.

LINE-1 is activated and readily retrotransposes in proliferating cells. Therefore, we first tested whether binge METH would activate LINE-1 in cells proliferating within the neurogenic zones. We found that, compared to the saline group, binge METH treatment can slightly increase immunoreactivity of Ki-67, a marker of proliferating cells, in the SGZ and SVZ (+9.22%, $p > 0.05$ and +21.5%, $^{*}p < 0.05$, respectively, n=6, by two-way ANOVA followed by Bonferroni post hoc test) at 24 hours after the last injection of the

drug (Fig. 3.4.A-C). We also found that some ORF-2 immunoreactivity co-localized with Ki-67 immunoreactivity (in the same compartment or cell type) in both saline and METH-treated rats (Fig. 3.4.A-B). Statistically, METH treatment did not significantly change co-localization of the ORF-2 signal with the Ki-67 signal in the SGZ and SVZ when assessed by Pearson's correlation analysis (+42.2%, $p > 0.05$; +17.9%, $p > 0.05$, respectively, n=6, by two-way ANOVA followed by Bonferroni post hoc test) (Fig. 3.4.C.b). This finding was not surprising as Ki-67 localizes mainly in the nucleus while ORF-2 localizes primarily in the cytoplasm. Therefore, we next counted the cells that expressed both proteins regardless of the sub-cellular compartment. As compared to the saline controls, the METH-treated rats expressed, on average, 19.2 cells (vs. 12.3 cells in saline group) that expressed both proteins in the SGZ, which was a 56.1% increase. In the SVZ, 7.63 cells (vs. 5.78 cells in saline group), on average, expressed both proteins in METH-treated rats, which translated to a 32.0% increase compared to the saline control (Fig. 3.5).

We used DCX as a marker of precursor (type-2b and type-3 cells) and immature neuronal cells to discover if neurotoxic binge METH could activate LINE-1 in any of these types of cells. As shown in our previous study [86], many but not all ORF-2-positive neurons were also positive for DCX in both the saline- and METH-treated rats (Fig.3.5). However, statistically, binge METH did not show a significant effect on the immunoreactivity of DCX in the SGZ and SVZ (+10.3%, $p > 0.05$, and +20.0%, $p > 0.05$, respectively, n=4, by two-way ANOVA followed by Bonferroni post hoc test) (Fig.3.6.A-C). Similarly, binge METH did not affect the co-localization of the ORF-2 signal with DCX signal in the SGZ and SVZ ($F(1,12) = 4.52$, $p > 0.05$, n = 4, by two-way ANOVA) (Fig.3.6.C.b). In addition to proliferating precursor cells and immature neurons, there are

mature neuronal and glial cells within the neurogenic zones. Immunostaining for NeuN, a classic marker of postmitotic neurons, revealed binge METH significantly decreased the immunoreactivity of NeuN in the SGZ and SVZ (-15.31%, ***$p<0.001$ and -38.15%, *$p<0.05$, respectively, n=6, by two-way ANOVA followed by Bonferroni post hoc test) (Fig. 3.7.C.a). At the same time, binge METH increased co-localization of the ORF-2 signal with the NeuN signal in the SGZ but not the SVZ compared to the saline group (+74.58%, **$p<0.005$, and +7.66%, $p > 0.05$, respectively, n=6, by two-way ANOVA followed by Bonferroni post hoc test) (Fig.3.7.b).

The ORF-2 signal did not co-localize with the MAP2 (marker of neuronal cells) signal in the cytoskeleton outside the neurogenic zones (Fig.3.8).

The result suggests that systemic administration of neurotoxic doses of binge METH increased the activity of LINE-1 in postmitotic neurons in the SGZ.

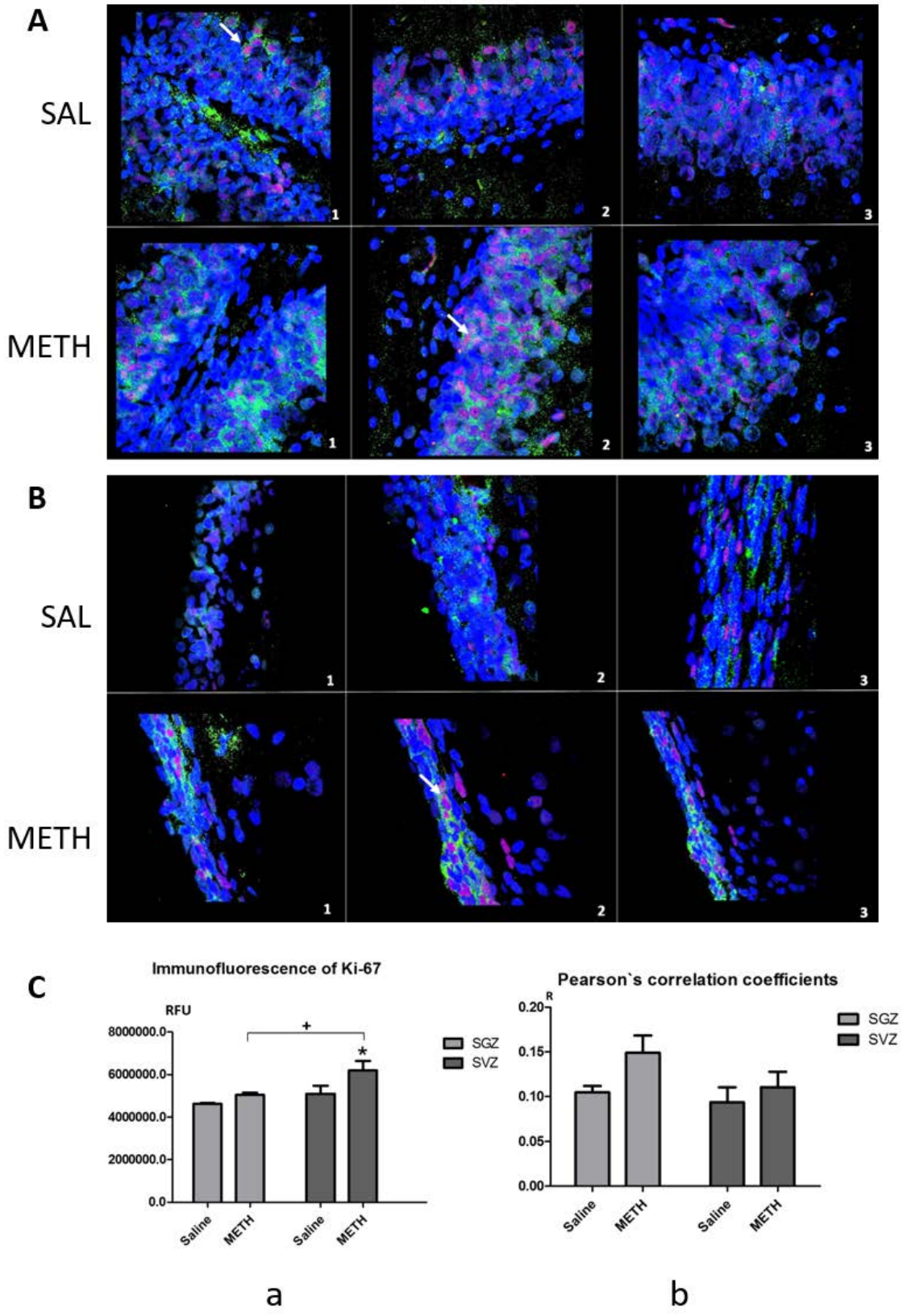
A
SAL
METH
1
2
3
B
SAL
METH
1
2
3
C
Immunofluorescence of Ki-67
RFU
8000000.0
6000000.0
4000000.0
2000000.0
0.0
+
*
SGZ
SVZ
Saline
METH
Saline
METH
a
Pearson`s correlation coefficients
R
0.20
0.15
0.10
0.05
0.00
SGZ
SVZ
Saline
METH
Saline
METH
b

Figure 3.4. Binge METH does not change immunoreactivity of Ki-67 in the neurogenic zones. Representative images from 3 regions of the SGZ (A) and the SVZ (B) per condition (SAL and METH) were taken. The Ki-67 protein signals (pink) showed increase in METH-treated rats compared to the saline-treated rats The two-way ANOVA showed significant effect in Ki-67 signal of treatment ($F(1,20) = 6.40$, $^*p < 0.05$, n=6) and region ($F(1,20) = 7.37$, $^*p < 0.05$, n=6). Bonferroni post-tests did not reveal significant difference in Ki-67 in SGZ but showed a significant increase in SVZ between treatment (+9.22%, $p > 0.05$, and +21.5%, $^*p < 0.05$, respectively, n=6). Bonferroni post-tests revealed a significant increase in Ki-67 in the saline-treated group but not the METH-treated group between SGZ and SVZ (+10.4%, $^*p < 0.05$, and +22.8%, $p > 0.05$, respectively, n=6). Some ORF-2-positive neurons (green) are positive for Ki-67 (arrows), which is a selective marker of proliferating cells, in both saline- and METH-treated rats. METH does not change co-localization of ORF-2 signal with Ki-67 signal in neurogenic zones. The two-way ANOVA did not show significant effect in co-localization of ORF-2 and Ki-67 of treatment ($F(1,20) = 2.47$, $p > 0.05$, n=6) & region ($F(1,20) = 3.72$, $p > 0.05$, n=6). The data are summarized in (C). Nuclei are depicted in blue. Abbreviations: METH, methamphetamine; SAL, saline; ORF-2; open reading frame 2; SGZ, subgranular zone; SVZ, subventricular zone.

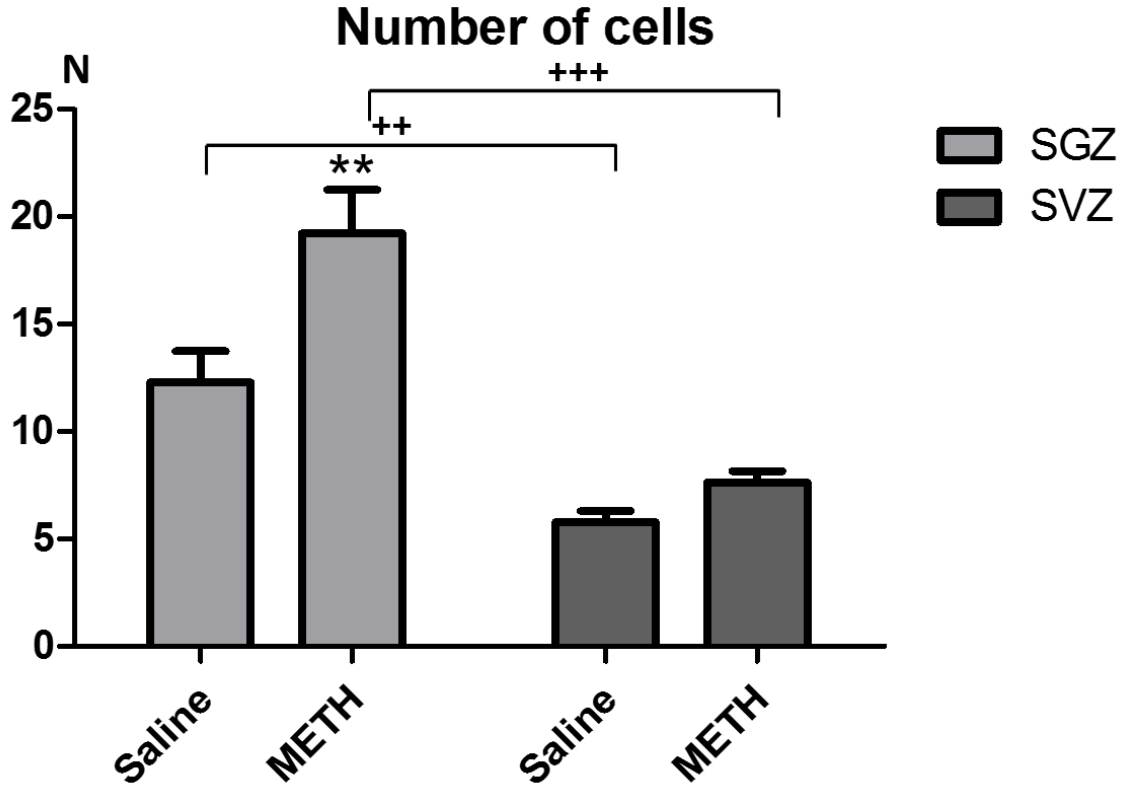

Figure 3.5. Number of cells expressing both ORF-2 immunoreactivity and Ki-67 immunoreactivity. The two-way ANOVA showed significant effect in number of cells that express both ORF-2 and Ki-67 of treatment ($F(1,20) = 49.2$, ***$p<0.001$, n=6) and region ($F(1,20) = 11.6$, **$p < 0.05$, n=6). Bonferroni posttests revealed a significant increase in SGZ but not SVZ between treatment (+56.1%, **$p < 0.005$, and +32.0%, $p > 0.05$, n=6). Bonferroni posttests revealed a significant increase in the saline-treated group and the METH-treated group between regions (-53.0%, **$p < 0.005$, and -60.3%, ***$p < 0.001$, respectively, n=6).—Nuclei are depicted in blue. Abbreviations: METH, methamphetamine; SAL, saline; ORF-2; open reading frame 2; SGZ, subgranular zone; SVZ, subventricular zone.

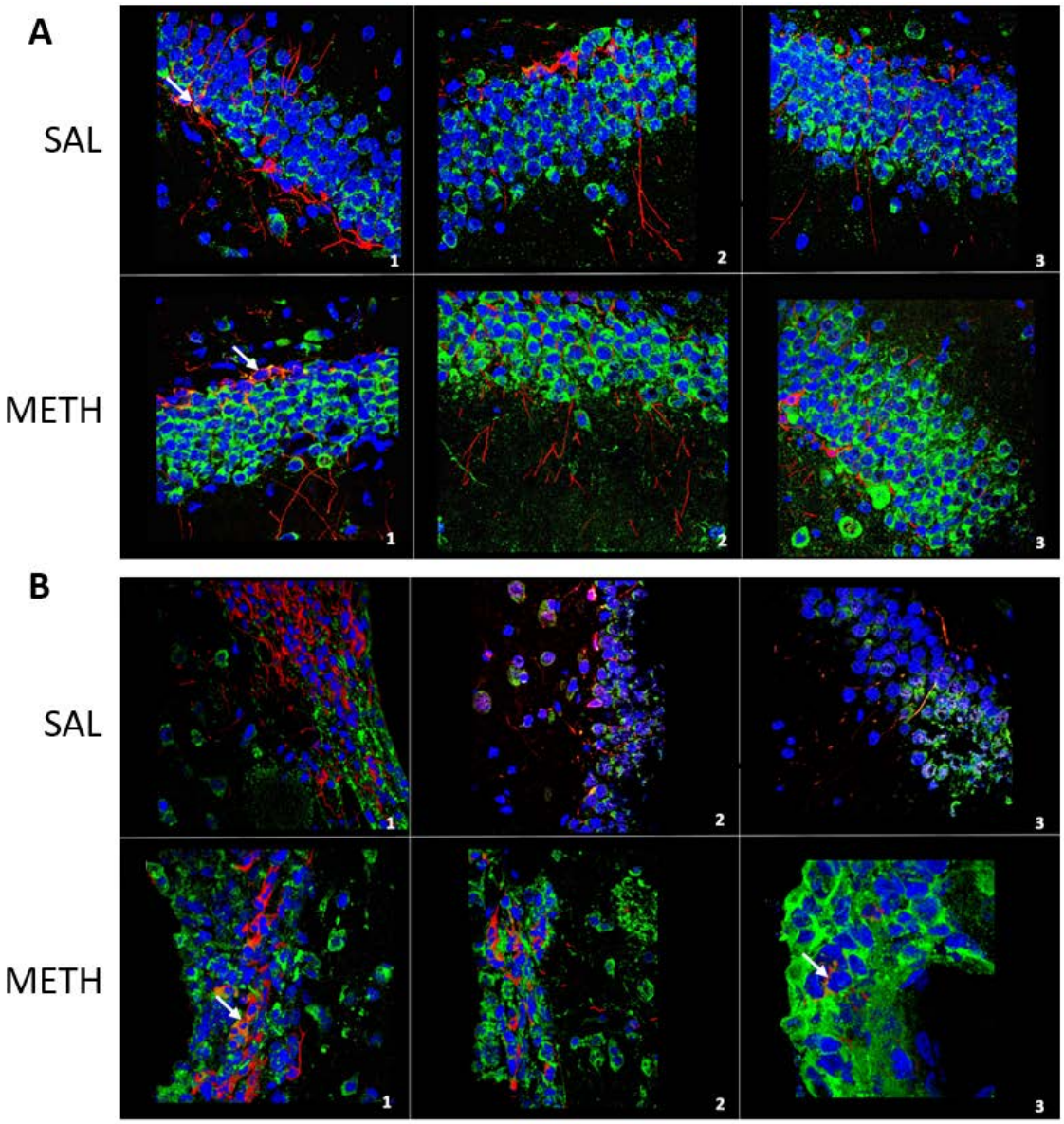
A
SAL
METH
1
2
3
B
SAL
METH
1
2
3
C
Immunofluoresence of DCX
RFU
1.0×10^07
8000000.0
6000000.0
4000000.0
2000000.0
0.0
Saline
METH
Saline
METH
a
Pearson's correlation coefficients
R
0.25
0.20
0.15
0.10
0.05
0.00
SGZ
SVZ
SGZ
SVZ
Saline
METH
Saline
METH
b

Figure 3.6. Binge METH has no effect on the immunoreactivity of DCX in the neurogenic zones. Representative images from 3 regions of the SGZ (A) and the SVZ (B) per condition (saline and METH) were taken. The two-way ANOVA showed a significant effect in DCX signal (red) of treatment ($F(1,12) = 11.3$, $^*p < 0.05$, n=4), but did not show significant effect in DCX signal of region ($F(1,12) = 1.01$, $p > 0.05$, n=4). Bonferroni posttests didn`t reveal significant difference in DCX signal in neither SGZ nor SVZ between treatment (+10.3%, $p > 0.05$, and +20.0%, $p > 0.05$, respectively, n=4)Some ORF-2-positive neurons (green) are also positive for DCX (arrows), which is a selective marker of immature and type-3 cells, in both the saline- and METH-treated rats. METH does not change co-localization of ORF-2 signal with DCX signal in the neurogenic zones The two-way ANOVA did not show significant effect in co-localization of ORF-2 and DCX of treatment ($F(1,12) = 4.52$, $p > 0.05$, n=4), but it showed a significant increase in region ($F(1,12) = 7.08$, $^*p < 0.05$, n=4). Bonferroni posttests didn`t reveal significant difference in DCX signal (red) in neither SGZ nor SVZ between treatment (+10.3%, $p > 0.05$, and +20.0%, $p > 0.05$, respectively, n=4). . The data are summarized in (C). Nuclei are depicted in blue. Abbreviations: METH, methamphetamine; SAL, saline; ORF-2; open reading frame 2; SGZ, subgranular zone; SVZ, subventricular zone.

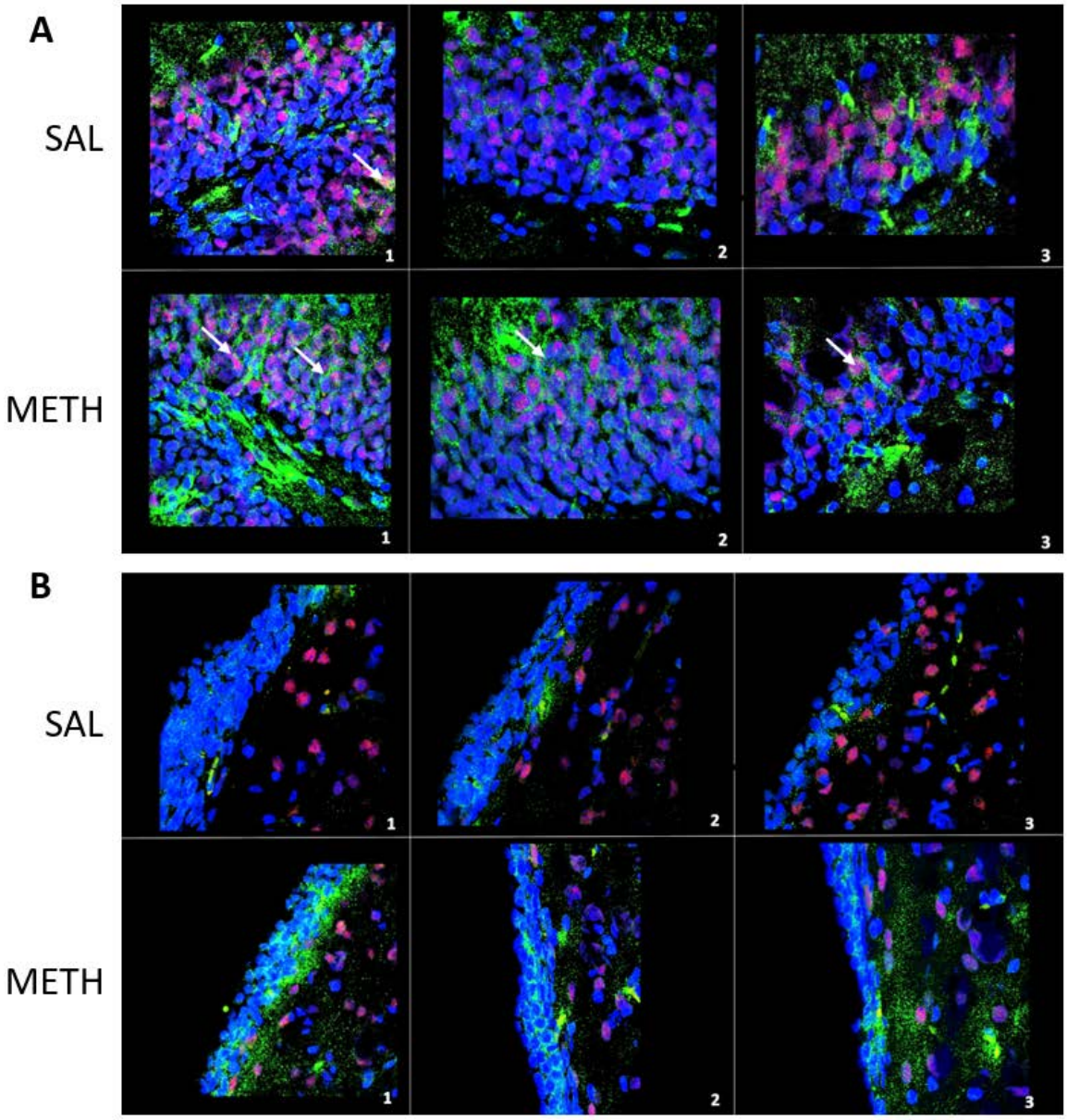
A
SAL
METH
1
2
3
B
SAL
METH
1
2
3
C
Immunofluorescence of NeuN
RFU
5000000
4000000
3000000
2000000
1000000
0
+
+++
***
***
SGZ
SVZ
Saline
METH
Saline
METH
a
Pearson`s correlation coefficients
R
0.6
0.4
0.2
0.0
+++
+++
**
SGZ
SVZ
Saline
METH
Saline
METH
b

Figure 3.7. Binge METH decreases the immunoreactivity of NeuN in the SGZ. Representative images from 3 regions of the SGZ (A) and the SVZ (B) per condition (saline and METH) were taken. The two-way ANOVA showed significant effect in NeuN signal (pink) of treatment ($F(1,20) = 1378$, ***$p < 0.001$, n=6) and region ($F(1,20) = 40.0$, *$p < 0.05$, n=6). Bonferroni posttests revealed a significant decrease in NeuN signal (pink) in SGZ and SVZ between treatment (-15.31%, ***$p < 0.001$ and -38.15%, *$p < 0.05$, respectively, n=6). Bonferroni posttests revealed a significant decrease in NeuN signal in the saline-treated group and the METH-treated group between SGZ and SVZ (-83.2%, ***$p < 0.001$ and -76.7%, ***$p < 0.001$, respectively, n=6).Some of ORF-2-positive neurons (green) are also positive for NeuN (arrows), a selective marker of mature neurons, in both the saline- and METH-treated rats. The two-way ANOVA showed a significant increase in co-localization of ORF-2 and NeuN of treatment ($F(1,20) = 77.1$, ***$p < 0.001$, n=6), and region ($F(1,20) = 15.00$, ***$p < 0.001$, n=6). Bonferroni posttests revealed significant increase in co-localization between ORF-2 and NeuN in SGZ but not SVZ after binge METH (+74.58%, **$p < 0.005$, and +7.66%, $p > 0.05$, respectively, n=6). Bonferroni posttests revealed significant increase in co-localization in the saline-treated group and the METH-treated group between regions (+152%, ***$p < 0.001$ and +72.0%, ***$p < 0.001$, respectively, n=6). The data are summarized in (C). Nuclei are depicted in blue. Abbreviations: METH, methamphetamine; SAL, saline; ORF-2; open reading frame; SGZ, subgranular zone; SVZ, subventricular zone.

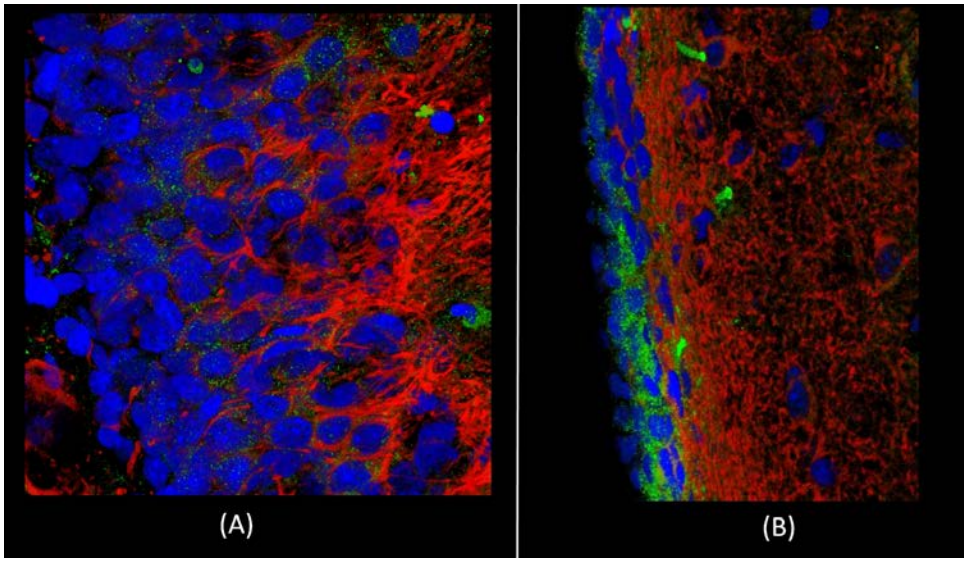

Figure 3.8. The ORF-2 signal does not co-localize with the MAP2 signal in cytoskeleton outside the neurogenic zones. METH (10 mg/kg free base) was administered to young adult male Sprague-Dawley rats every 2h in four successive intraperitoneal (i.p.) injections and the rats were killed 24h later. The ORF-2 signal (green) does not co-localize with the MAP2 signal (red) outside the SGZ (A) or SVZ (B) after METH treatment.

3.3.2. Radial glial-like stem cells and mature glial cells

Radial glia-like stem cells and mature glia both express GFAP protein; however, they differ in localization and shape. In the SGZ, radial glia-like cells reside at the bottom of the zone (adjacent to the hilus) and have small cell bodies with short processes, while mature glia reside mostly at the top and outside of the zone and are star-shaped with long processes (Fig.3.10). In the SVZ, radial glia-like cells are mostly located adjacent to the ventricle, while the majority of mature glia localize close to the striatum.

We have detected that binge METH increased the immunoreactivity of GFAP in the SGZ and SVZ and their immediate proximity (+44.6%, **$p < 0.005$ and +120%, ***$p < 0.001$, respectively, n=4, by two-way ANOVA followed by Bonferroni post hoc test). We also observed that most of the ORF-2 immunoreactivity co-localizes with GFAP immunoreactivity in both zones and METH treatment significantly increased the co-localization of both SGZ and SVZ (+85.3%, ***$p < 0.001$ and +130%, ***$p < 0.001$, respectively, n=4, by two-way ANOVA followed by Bonferroni *post hoc* test.) (Fig.3.9). The ORF-2 signal co-localized with the GFAP signal in both radial and mature glia in the DG (Fig.3.10).

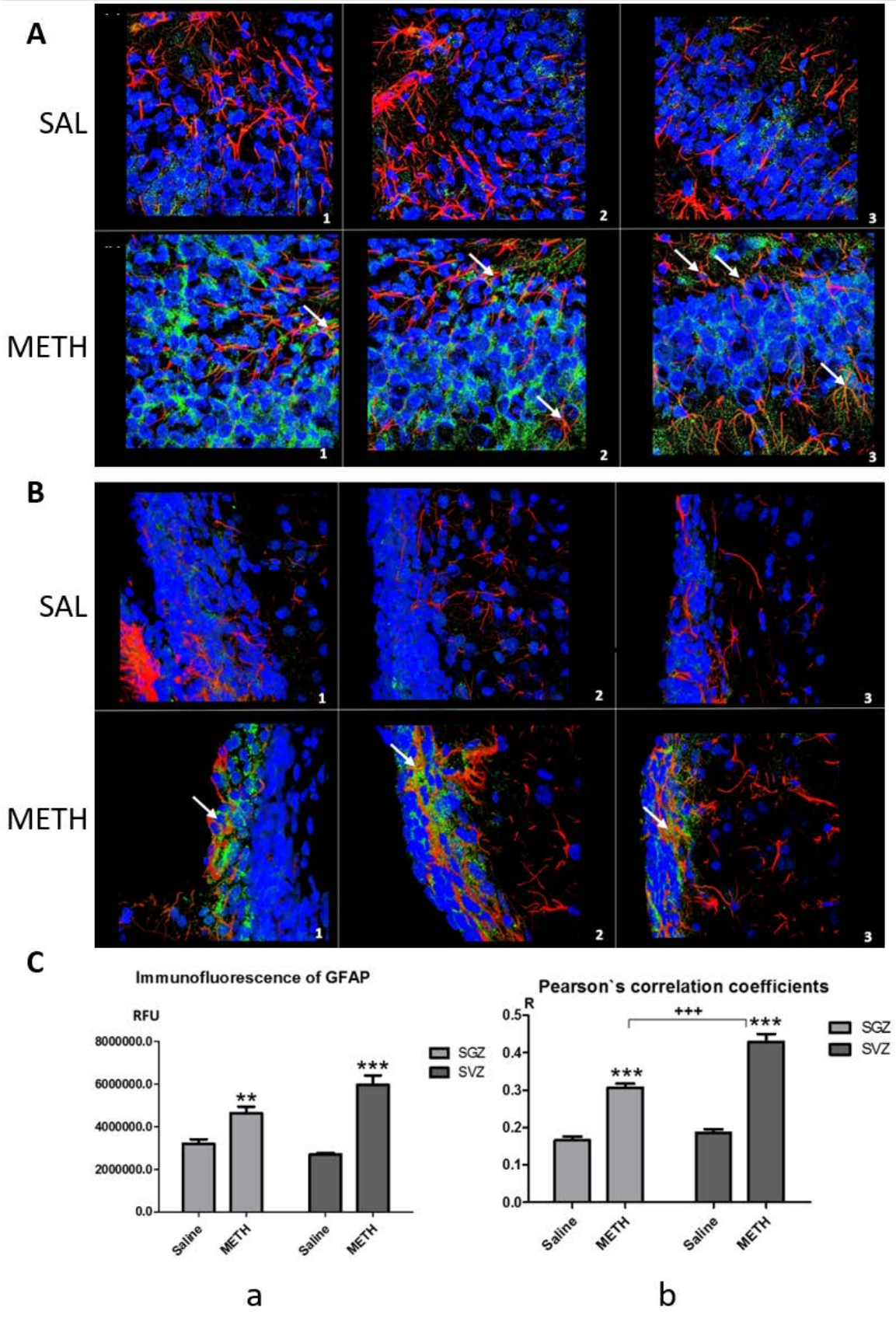
A
SAL
METH
1
2
3
B
SAL
METH
1
2
3
C
Immunofluorescence of GFAP
RFU
8000000.0
6000000.0
4000000.0
2000000.0
0.0
**
***
SGZ
SVZ
Saline
METH
Saline
METH
a
Pearson`s correlation coefficients
R
0.5
0.4
0.3
0.2
0.1
0.0
+++
***
***
SGZ
SVZ
Saline
METH
Saline
METH
b

Figure 3.9. Binge METH increases immunoreactivity of GFAP in the neurogenic zones. Representative images from 3 regions of the SGZ (A) and the SVZ (B) per condition (saline and METH) were taken. The two-way ANOVA showed a significant increase in GFAP signal (red) of treatment ($F(1,12) = 1.99$, ***$p < 0.001$, n=4) but not region ($F(1,12) = 63.7$, $p > 0.05$, n=4). Bonferroni posttests revealed a significant increase in GFAP signal in SGZ and SVZ between treatment (+44.6%, **$p < 0.005$ and +120%, ***$p < 0.001$, respectively, n=4). ORF-2-positive neurons (green) are also positive for GFAP (arrows), which is a selective marker of radio-glial-like and mature glial cells, in both the saline- and METH-treated rats. The two-way ANOVA showed a significant increase in co-localization of ORF-2 and GFAP of treatment ($F(1,12) = 27.9$, ***$p < 0.001$, n=4), and region ($F(1,12) = 201$, ***$p < 0.001$, n=4). Bonferroni posttests revealed a significant increase in co-localization between ORF-2 and GFAP in SGZ and SVZ after binge METH (+85.3%, ***$p < 0.001$, and +130%, ***$p < 0.001$, respectively, n=4). Bonferroni posttests did not reveal significant difference in co-localization in the saline-treated group between regions. But it showed a significant increase in the METH-treated group between SGZ and SVZ (+12.6%, $p > 0.05$ and +40.0%, ***$p < 0.001$, respectively, n=4). The data are summarized in (C). Nuclei are depicted in blue. Abbreviations: METH, methamphetamine; SAL, saline; ORF-2; open reading frame; SGZ, subgranular zone; SVZ, subventricular zone.

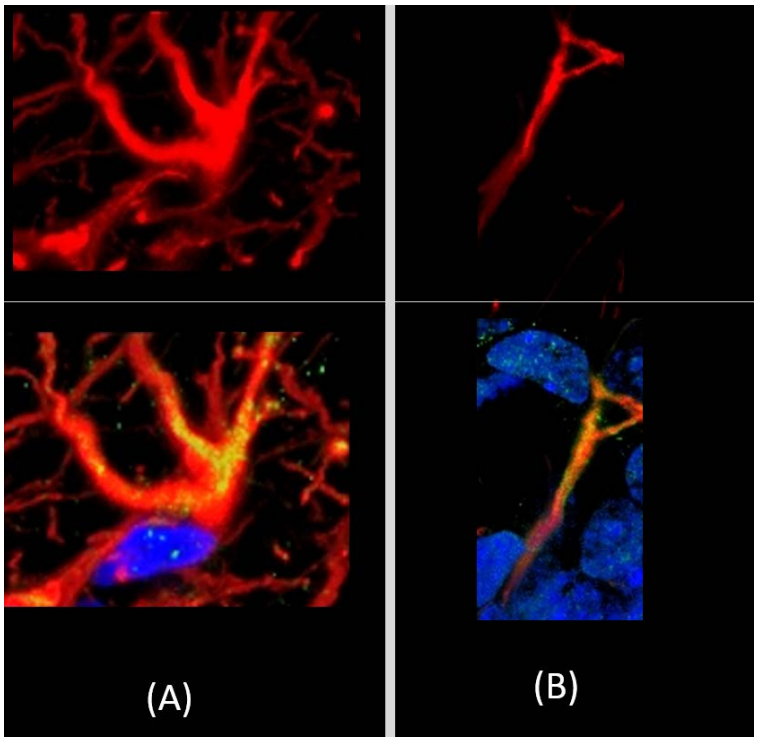

Figure 3.10. The ORF-2 signal co-localizes with the GFAP signal in different types of glial cells of the SGZ after METH exposure. METH (10 mg/kg free base) was administered to young adult male Sprague-Dawley rats every 2h in four successive intraperitoneal (i.p.) injections and the rats were killed 24h later. ORF-2 signal (green) signal co-localize with GFAP signal (red) in both mature glial cells (A) and radio-glial cells (B).

3.4. The Role of LINE-1 in the Neurogenic Zones

So far, we have demonstrated that systemic administration of neurotoxic doses of binge METH increases the activity of LINE-1 in glial cells and postmitotic cells in the neurogenic zones. We further investigated the role of increased ORF-2 in these types of cells. As mentioned before, administration of high doses of METH can cause oxidative stress, inflammatory response, and neuronal apoptosis, which lead to damage of DAergic and 5HTergic neuronal terminals (neurotoxicity). [137]. We would like to determine whether binge METH-induced increase of LINE-1-encoded ORF-2 protein is associated with apoptosis and/or oxidative stress. Therefore, we next stained the tissue using the markers specific for different stages of apoptosis and oxidative stress. We found that binge METH significantly increased immunoreactivity of cleaved caspase-3, which localized mostly in the nucleus, in the SGZ and SVZ (+71.4%, ***$p < 0.001$ and +92.3%, ***$p < 0.001$, respectively, n=4, by two-way ANOVA followed by Bonferroni *post hoc* test). This result was consistent with the existing knowledge that exposure to a high dose of METH induces apoptosis. Moreover, METH treatment can significantly increase the co-localization of ORF-2 immunoreactivity and cleaved caspase-3 immunoreactivity in the SGZ and SVZ (+25.2%, $p > 0.05$ and +68.42%, ***$p < 0.001$, respectively, n=4, by two-way ANOVA followed by Bonferroni *post hoc* test) compared to saline controls (Fig.3.11).

Commonly, cleaved caspse-3 localize in the cytoplasm. To verify the reliability of the cleaved caspase-3 antibody, we treated PC12 cells with glutamic, an acid-stress factor, and stained the cells with cleaved caspase-3 antibody. The cleaved caspase-3 was observed in the cytoplasm (Fig.3.12). Subsequently, we used cleaved PARP as a marker of late stage apoptosis and found that METH did not significantly increase the signal of cleaved PARP in the SGZ and SVZ (+22.3%, $p > 0.05$ and +18.7%, $p > 0.05$ respectively, n=6, two-way ANOVA followed by Bonferroni *post hoc* test). Furthermore, METH treatment did not change the co-localization of the ORF-2 signal and cleaved PARP signal in the SGZ and SVZ ($F(1,20) = 0.113$, $p > 0.05$, $n = 6$, by two-way ANOVA) (Figure 3.13). We also performed a triple staining study and found that the ORF-2 signal co-localizes with the cleaved-PARP signal in few immature (Figure 3.14) and proliferating (Figure 3.15) neuron cells within the neurogenic zones. All these results show that the ORF-2 signal co-localizes with some, but not all, apoptotic markers within the neurogenic zones after METH treatment, suggesting that METH-induced increases in ORF-2 may not be associated with apoptosis.

An increased level of GSH often indicates an adaptive response to oxidative stress. Interestingly, we found that binge METH significantly increased immunoreactivity of GSH in the SGZ and SVZ (+28.4%, $*p < 0.05$ and +46.9%, $p > 0.05n = 6$, by two-way ANOVA followed by Bonferroni *post hoc* test). METH also significantly increased co-localization of ORF-2 with GSH in the SGZ and SVZ (+24.6%, $***p < 0.001$and +57.7%, $***p < 0.001$, respectively, $n = 6$, by two-way ANOVA followed by Bonferroni *post hoc* test) (Figure 3.16). Our data also showed that the ORF-2 signal co-localized with the GSH signal in

most cells within the neurogenic zones. We can conclude that binge METH-induced increase of ORF-2 may be associated with responses to oxidative stress.

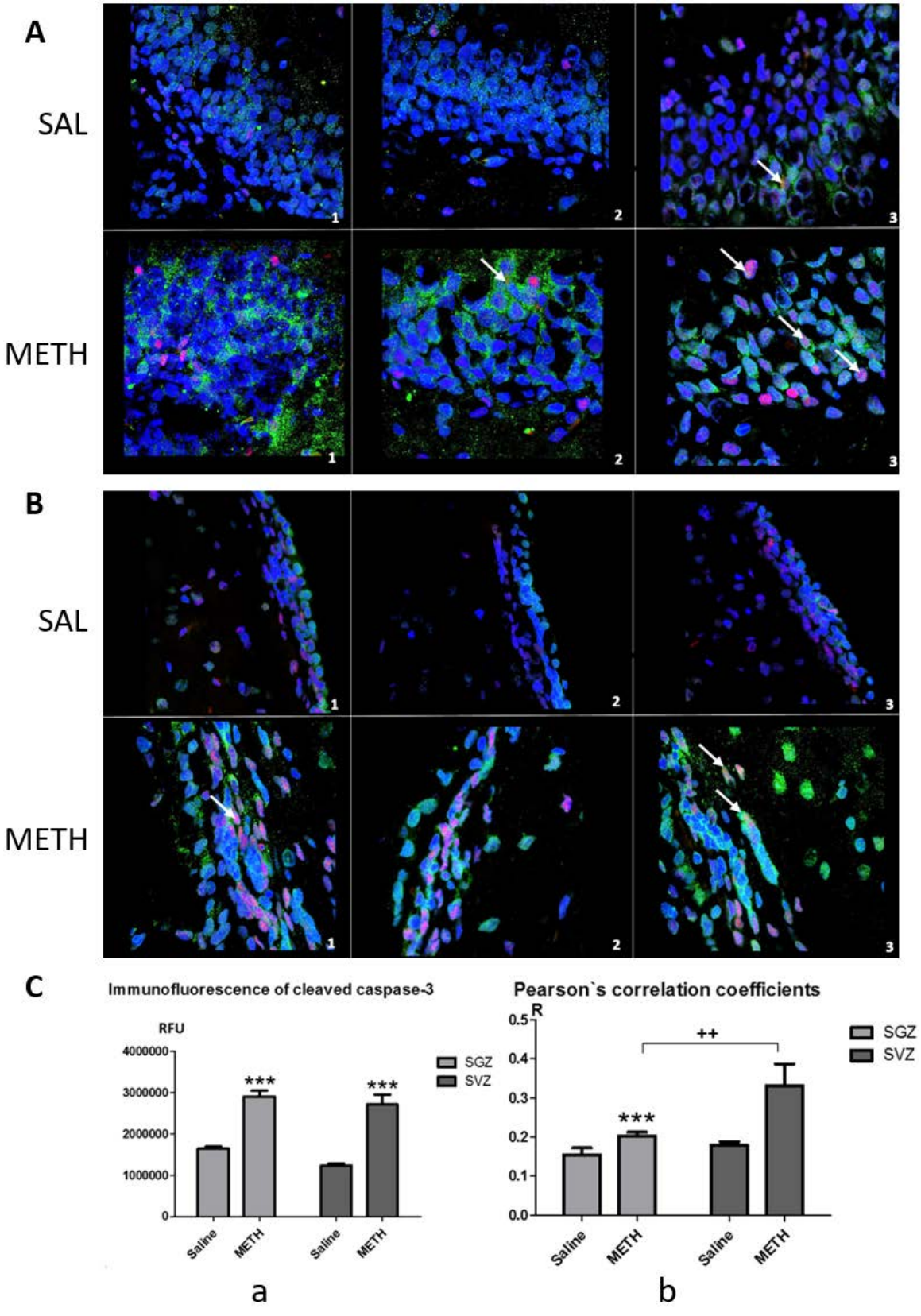
A
SAL
METH
1
2
3
B
SAL
METH
1
2
3
C
Immunofluorescence of cleaved caspase-3
RFU
4000000
3000000
2000000
1000000
0
***
***
SGZ
SVZ
Saline
METH
Saline
METH
a
Pearson`s correlation coefficients
R
0.5
0.4
0.3
0.2
0.1
0.0
++
***
SGZ
SVZ
Saline
METH
Saline
METH
b

Figure 3.8. Binge METH increases immunoreactivity of cleaved caspase-3 and ORF-2 immunoreactivity co-localizes with cleaved caspase-3 immunoreactivity in the neurogenic zones. Representative images from 3 regions of the SGZ (A) and the SVZ (B) (saline and METH) were taken. The two-way ANOVA showed a significant increase in cleaved caspase-3 signal (pink) of treatment ($F(1,12) = 87.8$, $^{***}p < 0.001$, n=4) but not region ($F(1,12) = 4.18$, $p > 0.05$, n=4). Bonferroni posttests revealed a significant increase in cleaved caspase-3 signal in SGZ and SVZ between treatment (+71.4%, $^{***}p < 0.001$ and +92.3%, $^{***}p < 0.001$, respectively, n=4).ORF-2-positive neurons (green) are also positive for cleaved caspase-3 (arrows), a selective marker of middle stage of apoptosis, in both the saline- and METH-treated rats. The two-way ANOVA showed a significant increase in co-localization of ORF-2 and cleaved caspase-3 of treatment ($F(1,12) = 12.4$, $^{**}p < 0.005$, n=4), and region ($F(1,12) = 24.8$, $^{***}p < 0.001$, n=4). Bonferroni posttests did not reveal significant increase in co-localization between ORF-2 and cleaved caspase-3 in SGZ but showed a significant increase in SVZ after binge METH (+25.2%, $p > 0.05$, and +68.4%, $^{***}p < 0.001$, respectively, n=4). Bonferroni posttests did not reveal significant difference co-localization of ORF-2 and cleaved caspase-3 in co-localization in saline between regions. But it showed a significant increase in METH between SGZ and SVZ (+18.7%, $p > 0.05$ and +50.3%, $^{**}p < 0.005$, respectively, n=4).The data are summarized in (C). Nuclei are depicted in blue. Abbreviations: METH, methamphetamine; SAL, saline; ORF-2; open reading frame; SGZ, subgranular zone; SVZ, subventricular zone.

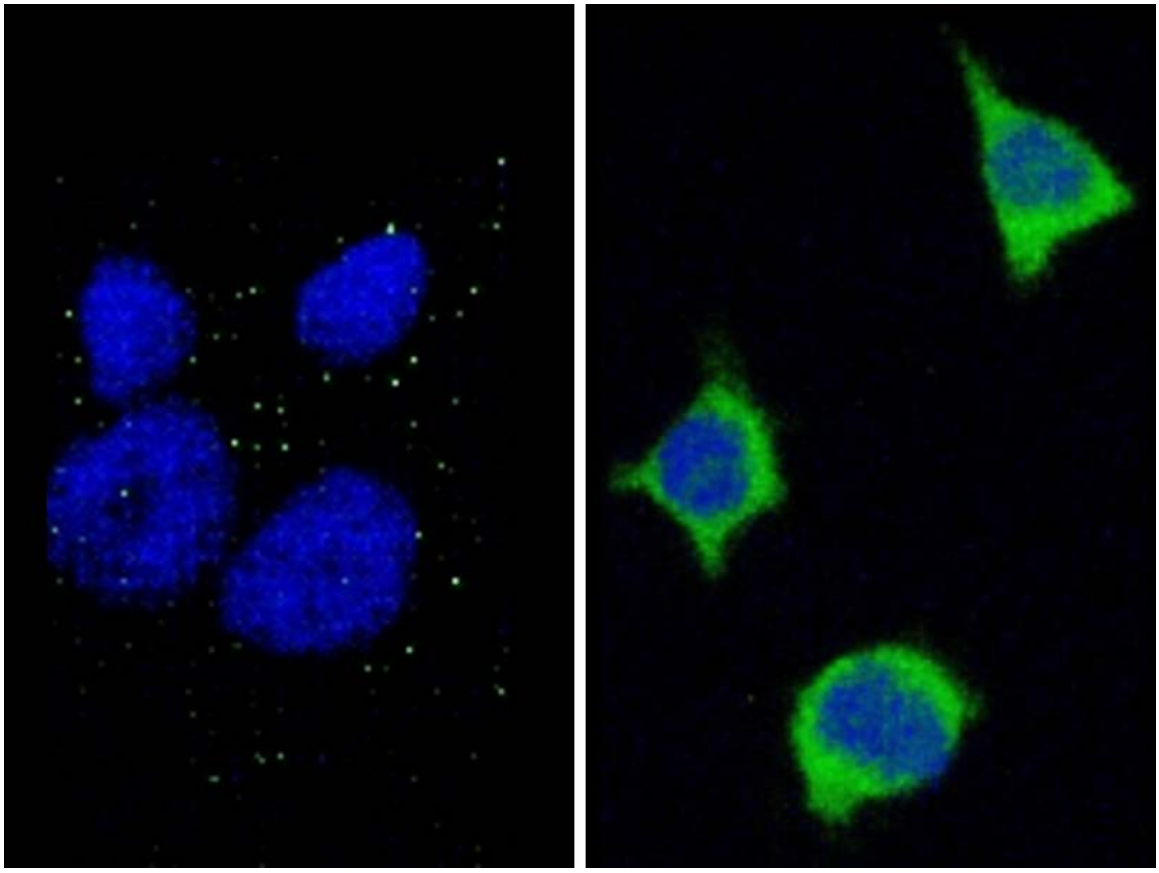

Figure 3.9. Cleaved caspase-3 immunoreactivity in PC12 cells. Cells were treated with 2mM glutamic acid for 4h (right) & untreated cells (left). After glutamic acid treatment,

cleaved caspase-3 (green) increases in the cytoplasm.

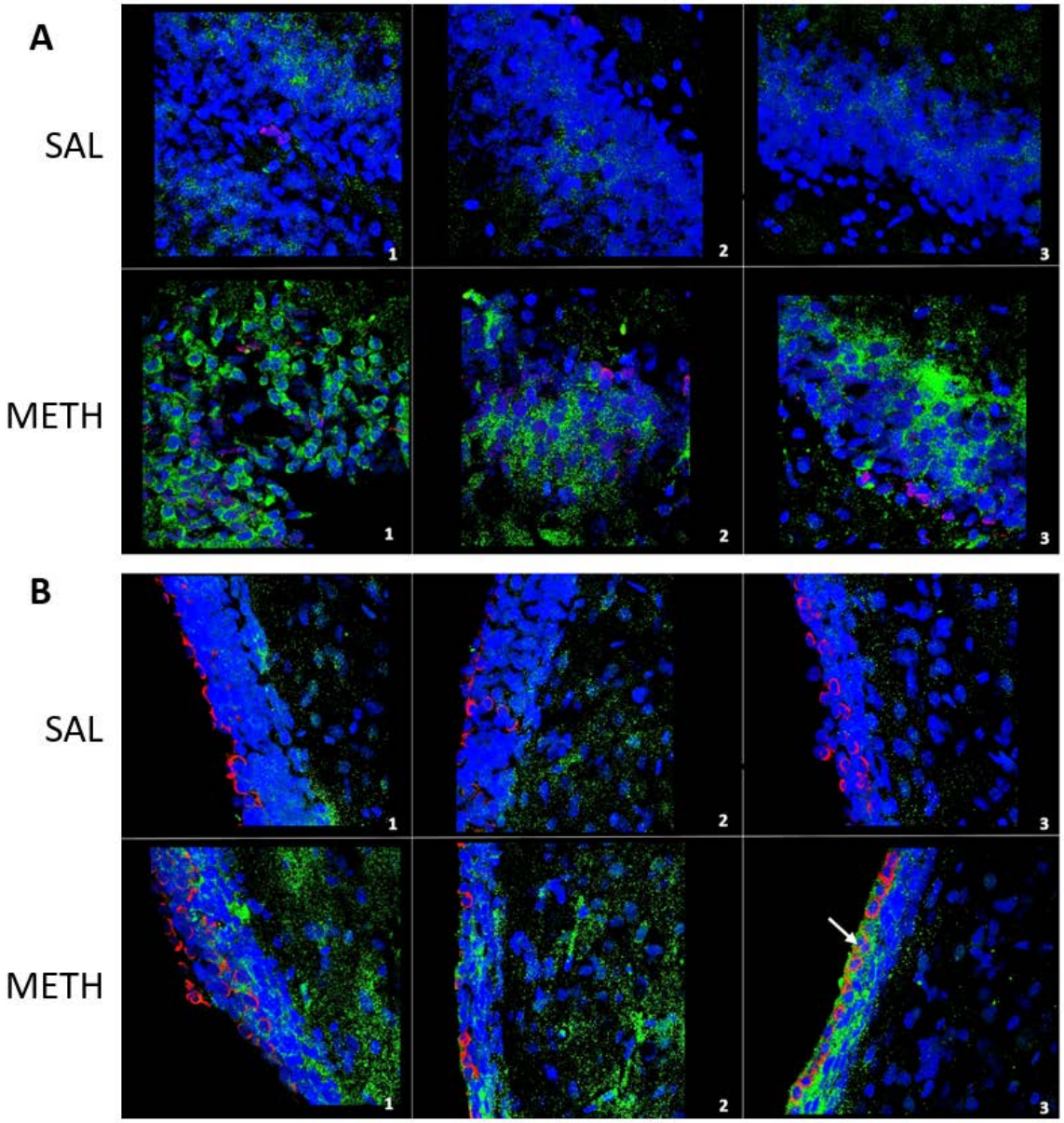
A
SAL
METH
1
2
3
B
SAL
METH
1
2
3

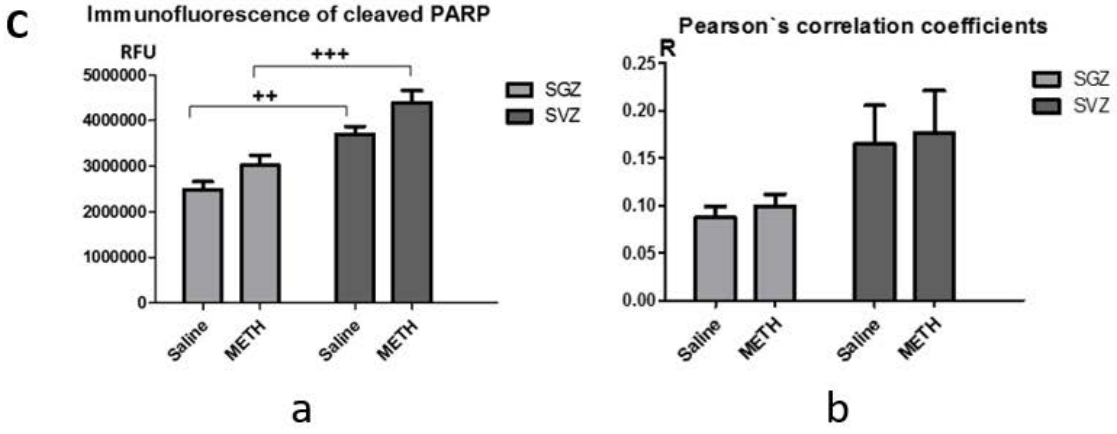
C
Immunofluorescence of cleaved PARP
RFU
5000000
4000000
3000000
2000000
1000000
0
++
+++
SGZ
SVZ
Saline
METH
Saline
METH
a
Pearson`s correlation coefficients
R
0.25
0.20
0.15
0.10
0.05
0.00
SGZ
SVZ
Saline
METH
Saline
METH
b

Figure 3.10. Binge METH increases immunoreactivity of cleaved PARP. ORF-2 signal co-localizes with cleaved PARP signal in the SVZ. Representative images from 3 regions of the SGZ (A) and the SVZ (B) (as shown in Figure3.2) per condition (saline (a) and METH (b)) were taken. The two-way ANOVA showed a significant increase in cleaved PARP signal (red) of treatment ($F(1,20) = 28.8$, $^{***}p < 0.001$, n=6) and region ($F(1,20) = 8.62$, $^{**}p < 0.005$, n=6). However, bonferroni posttests did not show significant difference in cleaved PARP signal in SGZ and SVZ between treatment (+22.3%, $p > 0.05$ and +18.7%, $p > 0.05$, respectively, n=6). Bonferroni posttests revealed a significant increase in cleaved PARP signal in the saline-treated group and the METH-treated one between regions (+48.8%, $^{**}p < 0.005$ and +45.6%, $^{***}p < 0.001$, respectively, n=6). ORF-2-positive neurons (green) were also positive for cleaved PARP(arrows) , which is a selective marker of the late stage of apoptotic cells, The two-way ANOVA did not show significant difference in co-localization of ORF-2 and cleaved PARP of treatment ($F(1,20) = 0.113$, $p > 0.05$, n=6). But it showed a significant increase in region ($F(1,20) = 6.04$, $^{*}p < 0.05$, n=6). Bonferroni posttests did not reveal significant increase in co-localization between ORF-2 and cleaved PARP in neither the saline-treated group nor the METH-treated group between regions (+87.6%, $p > 0.05$, and +78.3%, $p > 0.05$, respectively, n=6). The data are summarized in (C). Nuclei are depicted in blue. Abbreviations: METH, methamphetamine; SAL, saline; ORF-2; open reading frame; SGZ, subgranular zone; SVZ, subventricular zone.

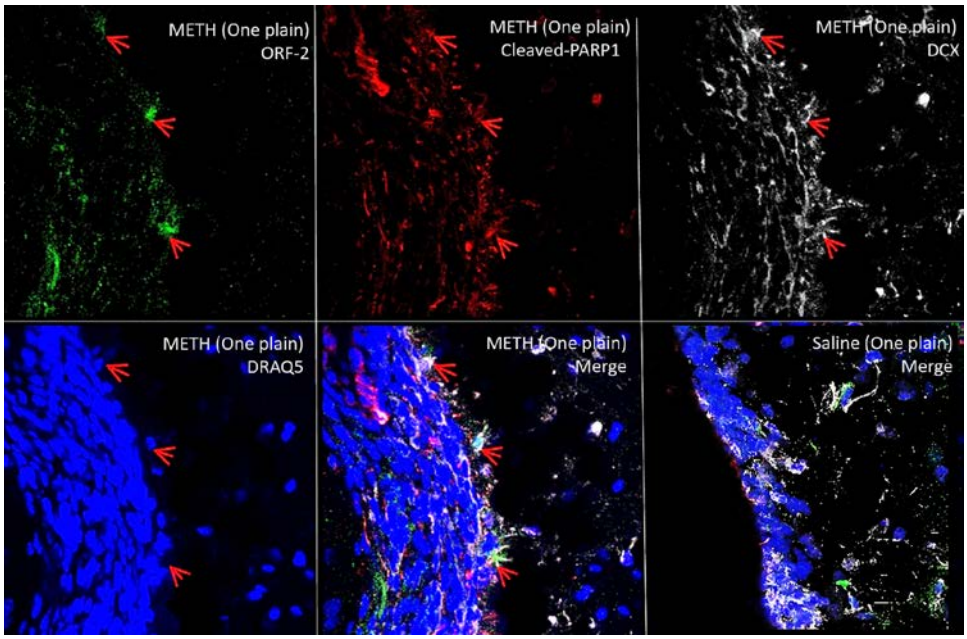

Figure 3.11. ORF-2 signal co-localizes with the cleaved-PARP signal in some immature neuron cells within the neurogenic zones. Single plain shows that ORF-2 signal (green) co-localizes with the cleaved-PARP signal (red) in some DCX (white) positive cells within the neurogenic zones after binge METH.

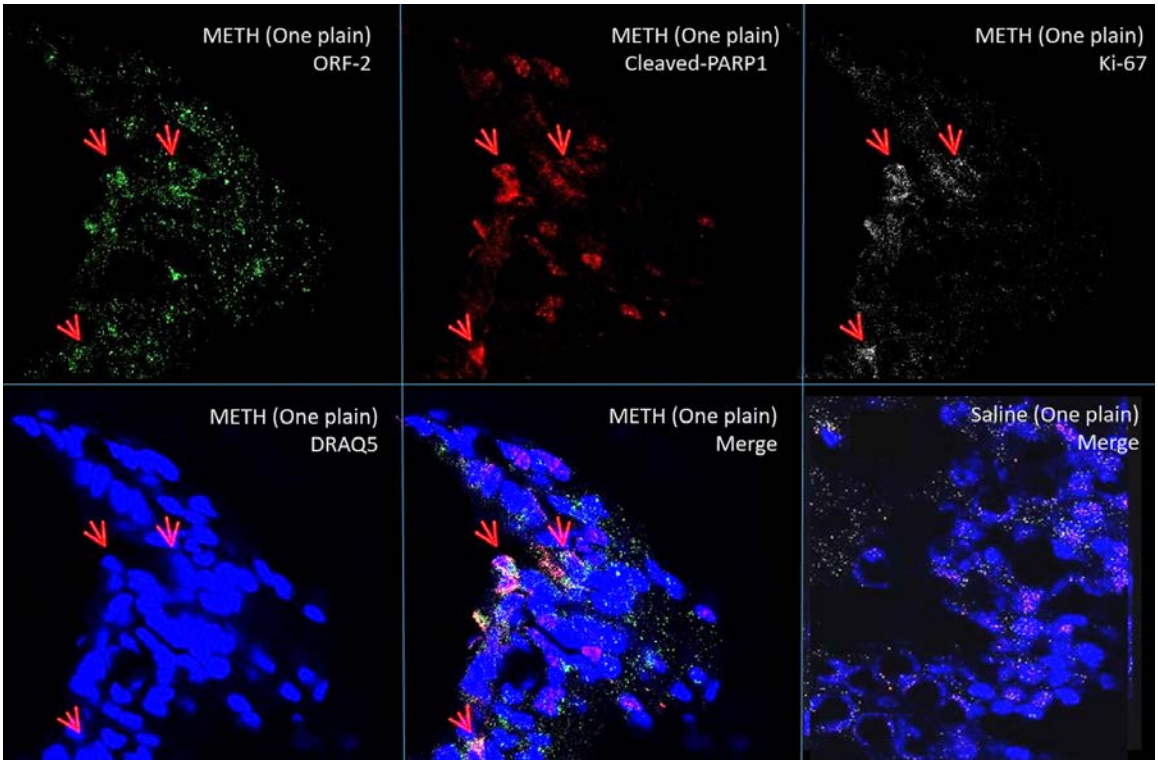

Figure 3.12. ORF-2 signal co-localizes with the cleaved-PARP signal in some proliferating neuronal cells within the neurogenic zones. Single plain shows that ORF-2 signal (green) co-localizes with the cleaved-PARP signal (red) in some Ki-67(white) positive cells within the neurogenic zones after binge METH.

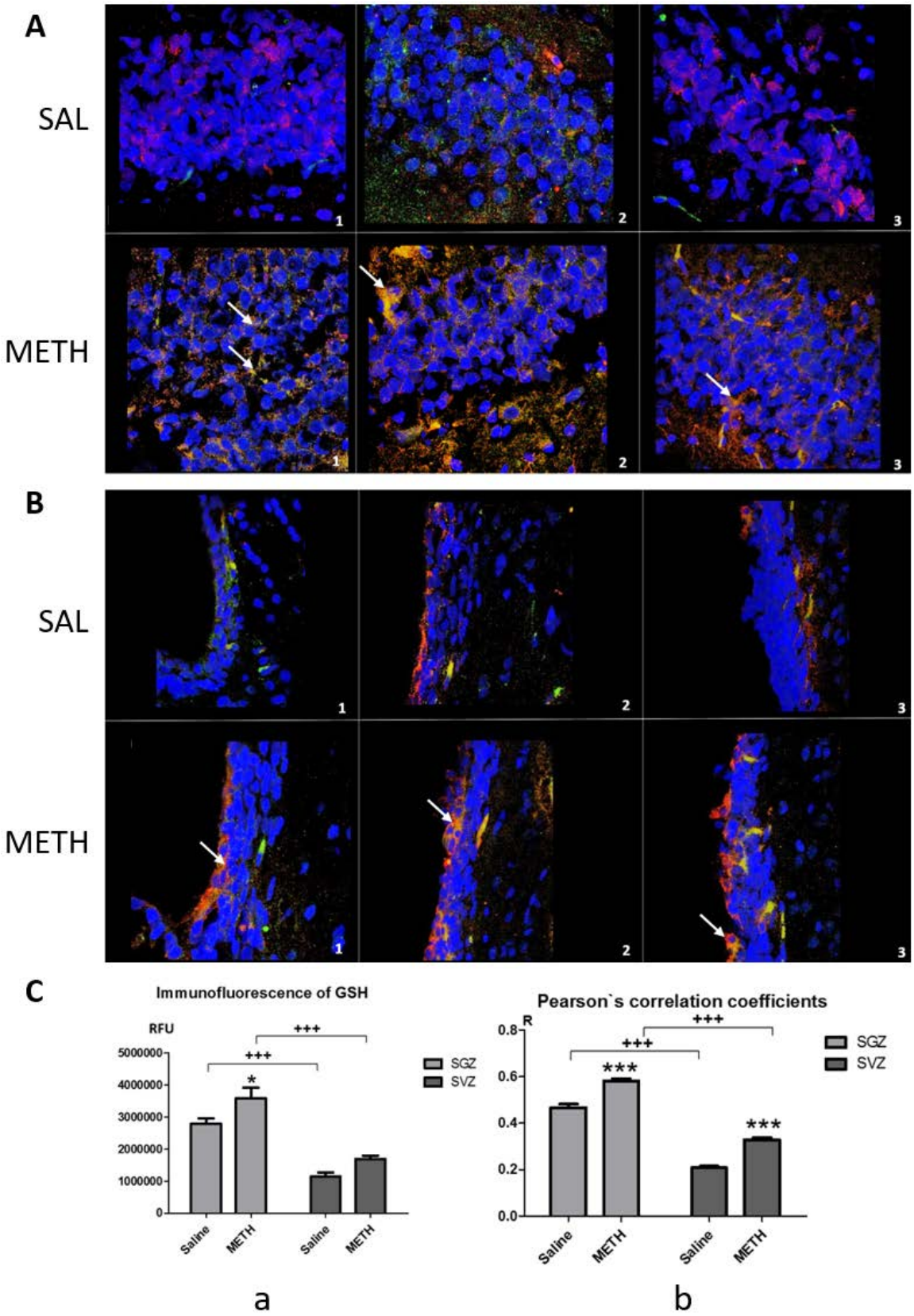
A
SAL
METH
1
2
3
B
SAL
METH
1
2
3
C
Immunofluorescence of GSH
RFU
5000000
4000000
3000000
2000000
1000000
0
+++
+++
*
SGZ
SVZ
Saline
METH
Saline
METH
a
Pearson`s correlation coefficients
R
0.8
0.6
0.4
0.2
0.0
+++
+++
***
***
SGZ
SVZ
Saline
METH
Saline
METH
b

Figure 3.13. Binge METH increases immunoreactivity of GSH. ORF-2 signal co-localizes with GSH signal in both SGZ and SVZ. Representative images from 3 regions of the SGZ (A) and the SVZ (B) (as shown in Figure3.2) per condition (saline (a) and METH (b)) were taken. The two-way ANOVA showed a significant increase in GSH signal (red) of treatment ($F(1,20) = 75.6$, $^{***}p < 0.001$, n=6) and region ($F(1,20) = 10.7$, $^{**}p < 0.005$, n=6). Bonferroni posttests showed a significant increase in GSH signal in SGZ but not SVZ between treatment (+28.4%, $^{*}p < 0.05$ and +46.9%, $p > 0.05$, respectively, n=6). Bonferroni posttests revealed a significant decrease in GSH signal in the saline-treated group and the METH-treated group between SGZ and SVZ (-58.9%, $^{***}p < 0.001$ and -52.9%, $^{***}p < 0.001$, respectively, n=6). Some ORF-2-positive neurons (green) were also positive for GSH (arrows) (red), which is a selective marker of oxidative stress, in both saline- and METH-treated rats. The two-way ANOVA showed a significant increase in co-localization of ORF-2 and GSH of treatment ($F(1,20) = 584$, $^{***}p < 0.001$, n=6), and region ($F(1,20) = 124$, $^{***}p < 0.001$, n=6). Bonferroni posttests revealed a significant increase in co-localization between ORF-2 and GSH in both SGZ and SVZ between treatment (+24.6%, $^{***}p < 0.001$, and +57.7%, $^{***}p < 0.001$,, respectively, n=6). Bonferroni posttests revealed a significant decrease in co-localization between ORF-2 and GSH in both the saline-treated group and the METH-treated group between SGZ and SVZ (-55.4%, $p > 0.05$, and -43.8%, $p > 0.05$, respectively, n=6). The data are summarized in (C). Nuclei are depicted in blue. Abbreviations: METH, methamphetamine; SAL, saline; ORF-2; open reading frame; SGZ, subgranular zone; SVZ, subventricular zone.

Chapter 4 DISCUSSION

4.1. Binge METH Increases ORF-2 Protein Levels in the Neurogenic Zones

As demonstrated earlier, LINE-1 is a repetitive DNA retrotransposon, which can be activated and inserted into a genome by a copy-and-paste genetic mechanism [95]. It encodes two proteins; one protein is ORF-1, an RNA-binding protein, and the other is ORF-2, an endonuclease and reverse transcriptase. Both proteins are required for LINE-1 retrotransposition, and increase of the proteins can serve as a sign of LINE-1 activation. In this study, we used the increased level of ORF-2 protein as the sign of LINE-1 activation. We observed that binge METH can increase the ORF-2 protein level in the neurogenic zones, suggesting the LINE-1 activation. These results confirm our previous findings. Our group has reported previously that increased levels of ORF-2 were observed in the SGZ and SVZ at 24 hours after the last dose of binge METH [86], suggesting that METH-triggered LINE-1 activation in the cells residing in the neurogenic zones. Earlier studies indicated that LINE-1 is active in very early embryogenesis, and the insertion of LINE-1 has been detected in neoplastic cells [138, 139]. In normal adult somatic cells, with exception of germ cells, LINE-1 is typically quiescent within the genomes of mammals [140]. Moreover, there is both evidence for transposition of LINE-1 in neurons [141] and evidence for LINE-1 activation in the SGZ [134]. Most importantly, cellular stresses such as thermal, oxidative, and genotoxic stress can induce LINE-1 activation [142, 143] because neurotoxic doses of binge METH cause hyperthermia as well as oxidative damage to proteins, lipids, and DNA [9, 144].

4.2. Identification of Cell Types Expressing Activated LINE-1 in the Neurogenic Zones after Binge METH

4.2.1. Intermediate progenitor cells and neuronal cells

In our previous study [86], after binge METH, ORF-2 increased in both DCX-positive and DCX-negative cells in the SGZ and SVZ. Doublecortin is a microtubule-associated protein expressed in type-2b, type-3, and immature granule cells. Therefore, previous results indicated LINE-1 activation in neuronal precursors was not only differentiating and maturing into neurons but also in other cell types.

To identify additional cells types in which ORF-2 expression is increased after binge METH in the neurogenic zones, we used two neuronal markers (NeuN, MAP2) and a marker of proliferating cells (Ki-67) in this study. Firstly, to confirm the previous results, we stained the tissue with ORF-2 and DCX. We found that the level of DCX remained the same at 24 hours after binge METH. It has been reported that METH (10 nM) can increase DCX protein levels, suggesting a potentially enhanced neuronal differentiation. In the same study, the results also demonstrated that METH altered DG stem cell properties by delaying the cell cycle and decreasing self-renewal capacities [84]. However, another study showed that METH had a negative impact on SVZ stem/progenitor cells, inducing cell death and inhibiting neurogenesis. Specifically, METH decreased neuronal differentiation and maturation at non-toxic concentrations (1-10nM) [135]. In our study, the non-changed level of DCX could be explained by the supposition that the suppression of cell proliferation or differentiation occurred earlier or later than 24 hours after binge METH. Alternatively, it is also possible that initially METH did increase cell differentiation in the SGZ and SVZ but later caused the death of differentiating cells which masked the increase. This possibility is supported by the results of triple staining for DCX, cleaved PARP, and ORF-2. Only some DCX and cleaved PARP double-positive cells express ORF-2, suggesting

that METH treatment may promote death of DCX-positive cells in the neurogenic zones. To explain this discrepancy, an *in vitro* study in PC12 cells may be necessary to further determine the timeline of METH effects in cell proliferation. Our results are in agreement with the results of the Muotri group [141]. They found that engineered LINE-1 retrotransposed in differentiated neuronal precursors derived from rat hippocampus neural stem cells. Regarding the effect of binge METH on DCX levels, our finding- that there was no difference between the saline and METH rats, agrees with Mandyam's group's results, who found that intermittent access to METH self-administration had no effect on the number of DCX-positive cells in the SGZ [134]. Collectively, these data suggest that METH has a different effect on DCX-positive cells in the SGZ, depending on the dose, frequency of administration, and stage of cell differentiation.

Recent studies have disclosed that METH induces a reduction of proliferation in both the SVZ and the SGZ [145, 146]. In our study, however, a slight increase of Ki-67 was observed in the SVZ at 24 hours after binge METH administration. It has been reported that acute injection of METH produced a rapid and transient (lasting 7 days) decrease in the number of BrdU-positive cells in the rat striatum, but it had no effect on cells in the SVZ or DG [147]. Similarly, it was found that acute treatment with METH (25 mg/kg; i.p.) suppressed the proliferation of granule cells in the DG of adult gerbils, and this effect was transient (the proliferation rate was restored 36 hours after the drug challenge) [148]. Dr. Mandyam's group studied proliferation of progenitors using Ki-67 labeling in rats intravenously self-administering METH for an extended access (6 h/day: long access (LgA)) or limited access (1 h/day: short access (ShA)). They found that four sessions of LgA METH enhanced proliferation while 42 sessions of ShA and LgA METH reduced

proliferation [149]. Their group also found that when adult rats were given intermittent (occasional) access to METH for 1 hour twice a week, an initial pro-proliferative effect was produced, but opposing effects on late progenitors and postmitotic neurons resulted in no overall change in neurogenesis [150]. These findings demonstrate the dynamic regulation of neurogenesis by METH, and underscore how diverse durations of METH access alter distinct aspects of neurogenesis.

We did not find a significant difference of co-localization of ORF-2 and Ki-67 between saline and METH treatment using Pearson`s correlation coefficient. However, via manually counting the ORF-2 and Ki-67 double positive cells, a significant increase of the double positive cells in the neurogenic zone was observed in the METH treated group. Banaz`s group transfected porcine aortic endothelial (PAE) with a LINE-1 expression vector and generated cell clones harboring retrotransposition events. They demonstrated that LINE-1 retrotransposition events lead to the reduction of endothelial cell proliferation and migration in a PAE cell mode [151]. Fan’s group structured a siRNA expression vector for the LINE-1 ORF-1 encoding sequence and transfected hepatocellular carcinoma cells (Bel-7402, SMMC-7721, HepG2) and immortalized hepatocellular cells (LO2). They found that the transfection of a LINE-1 ORF-1p siRNA expression vector can efficiently reduce the expression of LINE-1 ORF-1 protein detecting by Western blot, and the decrease of LINE-1 ORF-1 protein inhibited the proliferation of the above cells on the third day (FENG Fan; Regulatory effect of LINE-1 ORF-1p on hepatocellular carcinoma cells and proliferation of immortalized hepatocellular cells; Medical Journal of Chinese People's Liberation Army 2012-03). However, Li’s group found that overexpression of LINE-1 ORF-1 protein promoted human colorectal cancer LoVo cell proliferation, and the

proliferation of LoVo cells can be inhibited by knocking down the LINE-1 protein using siRNA against LINE-1. The *in vivo* data revealed that LINE-1 ORF-1 protein overexpression promoted LoVo tumor growth in nude mice, whereas the siRNA knockdown of endogenous LINE-1 ORF-1 protein inhibited tumor growth. These results indicated that LINE-1 ORF-1protein could promote LoVo cell proliferation and invasion both *in vitro* and *in vivo* [152]. Those evident revealed that proliferation accompanies LINE-1 activation, which supported our results. However, both double staining and triple staining showed that only some ORF-2 positive cells are indeed proliferating cells.

Regarding mature neurons, we found that binge METH decreases the expression of NeuN in the neurogenic zones. Moreover, we did not find a decrease in DCX-positive neurons. Therefore, it is possible that some of the mature neurons died as a result of binge METH neurotoxicity. Previous studies have shown that METH can not only dysregulate neurogenesis but also induce apoptosis, which was followed by death of pyramidal and granule neurons [133, 134]. There are studies that have demonstrated that METH treatment can induce cell death of calbindin-containing GABA interneurons within the hippocampus in animal models [45, 47]. Our result further supports the conclusion that binge METH induces apoptosis in the neurogenic zones. Since ORF-2 was not enriched in DCX-positive cells, the results suggest that ORF-2 was activated in mature granule neurons by binge METH, and that the mature neurons were more susceptible to the effects of neurotoxic METH doses than differentiating and immature neurons.

There is some evidence indicating that LINE-1 is activated in mature cells under certain circumstances. For example, LINE-1 retrotransposition has been found in mature endothelial cells in addition to endothelial progenitors [151]. Higher LINE-1 DNA

methylation levels in the cumulus cells of mature oocytesin Polycystic Ovary Syndrome (PCOS) patients than control patients, have been observed. But there was no difference in the methylation of cumulus cells in immature oocytes between PCOS and control patients. Muotri's group first discovered that LINE-1 is capable of retrotransposition in these cells that also expressed the neuronal marker NeuN [141]. Garcia-Perez's group further demonstrated for the first time that engineered LINE-1 can retrotranspose efficiently in mature nondividing neuronal cells. Thus, these findings have proved that the degree of somatic mosaicism and the impact of LINE-1 retrotransposition in the human brain may be higher than previously thought [153]. However, there is no study testing LINE-1 level in mature cells after METH administration. Here, we found that increased amounts of ORF-2 and NeuN double positive cells were observed in neurogenic zones after METH treatment. The possible reasons why we did not see much co-localization between ORF-2 and NeuN in SVZ follow. Firstly, there are fewer mature neuron cells in the SVZ compared with the SGZ, based on our staining. There are primarily three cell types in the SVZ: type-A, type-B, and type-C cells. Type-B cells have characteristics of astrocytes and have the potential to generate type-C cells, which are the transit-amplifying progenitor cells. The type-C cells can further produce type-A cells, which are migrating neuroblasts. Therefore, there is a limited number of mature neuron cells in the SVZ. The SVZ has new GABA- and DA-containing interneurons and these neurons can migrate to the olfactory bulb in most adult mammals[154]. METH has been reported to induce apoptosis in these interneurons [155-157]. According to our data, most NeuN positive cells are located in the portion of the striatum adjacent to the SVZ but not within the SVZ. Secondly, there are many types of

mature neuronal cells in the brain. It is possible that LINE-1 only retrotransposes in certain types of mature neuron cells.

Microtubule-associated protein2 is one of the most frequently used markers for mature neurons [158, 159], which can stain the whole cell body. Therefore, we used MAP2 to determine whether LINE-1 affects the cytoskeleton. However, we did not detect the co-localization between ORF-2 and MAP2 signals in the cytoskeleton, which indicated that METH-related increases in ORF-2 may not be expressed in the cytoskeleton.

4.2.2. Radial glial-like stem cells and mature glial

METH has been reported to trigger inflammatory responses in areas where DA and 5-HT terminals are damaged. METH affects glial cell (e.g., microglia and astrocytes) activity. On the other hand, glial cell activity can modulate the neurotoxic and addictive effects of METH [55, 56]. Goncavalez and colleagues found that massive METH doses (30 mg/kg) increased GFAP levels in the hippocampi of mice [160]. We found a similar result, that binge METH increased expression of GFAP in the neurogenic zones and neighboring CA1-3 regions, which was likely due to METH's neurotoxic effects. So far there is no data on testing LINE-1 levels in glial cells after METH administration. Our observation that many GFAP-positive cells were also positive for ORF-2 suggested that ORF-2 may be mediating the inflammatory response in the hippocampi of binge METH-exposed rats. The Muotri group's results indicated that the glial cells did not support high levels of retrotransposition because there was no LINE-1 detected in S100-β-positive [141]. However, they discussed that they could not conclude that LINE-10eGFP transgene was silencing in glia based on their limited results. Another *in vitro* experiment based on an engineered LINE-1 reporter indicated that glia may support less LINE-1 mobilization than

neurons. They transfected human fetal brain stem cells (hCNS-SCns) with an expression construct containing a retrotransposition-competent human LINE-1 driven from its native promoter, which consisted of a reversed copy of the enhanced green fluorescent protein (EGFP) expression cassette. They found EGFP-positive cells can preferentially differentiate into glial cells rather than neurons [103]. There is another observation in human postmortem tissues that suggests LINE-1 retrotransposition events occur more often in neurons than in glia [161, 162]. Upton's group performed single-cell retrotransposon capture sequencing (RC-seq) on individual human hippocampal neurons and glial cells. They obtained a mean true positive estimate of 6.5 insertions per glial cell, based on the PCR validation rate determined for hippocampal neurons (45.0%). This rate was 52.6% lower than the estimated 13.7 insertions for hippocampal neurons. This result means that LINE-1 insertions can arise in proliferating neural stem cells prior to glial or neuronal commitment, while glial otherwise support less LINE-1 mobilization than neurons. However, our result showed that ORF-2 level increased significantly in GFAP-positive cells after METH administration, both in mature astrocytes outside the SGZ and SVZ, and in gasket cell within the SGZ and SVZ. To explain this, first of all, we must admit that the result of an *in vitro* study may be different than an *in vivo* study. Secondly, GFAP is a specific marker for mature astrocytes, but it is also a marker of the radial-glia-like type-1 cells which may limit its use in differentiating the cellular population [163]. It is necessary to distinguish radial glia-like cells and mature glial cells. These two types of cells are different in structure: radial glia-like cells are more like tadpoles, while glial cells have a star-like morphology. As mentioned before, they also have different locations. From our data, ORF-2 level increased in both types of cells, which may dilute the real influence

between glial cells and LINE-1 activation. To solve this problem, we could use another marker of glial cells in a future study. For example, S100β is another specific marker for mature astrocytes. We could use S100β to further confirm if LINE-1 increases in astrocytes after binge METH. Because METH causes activation of gliosis in the striatum, cortex, and hippocampus [55, 56] and we also observed increased ORF-2 immunofluorescence co-localizing with GFAP immunofluorescence in both the SGZ and SVZ, it is possible that METH-induced LINE-1 activation without subsequent retrotransposition may be associated with gliosis.

Enhanced gliogenesis is another reason for the observation of increased GFAP. Gliogenesis is the generation of glial cells from progenitors and precursor cells. Dr. Mandyam's group observed that intermittent 1 hour access to METH (I-ShA) and voluntary exercise increased gliogenesis in the medial prefrontal cortex [164]. They discussed that an I-ShA-induced proliferative environment may be attributable to changes in endogenous levels of neurotransmitters in the medial prefrontal cortex, especially DA, in which activation of distinct DA receptors have been pro-proliferative [165]. The voluntary exercise-induced pro-proliferative environment is possibly attributable to changes in vasculature and increased expression of endogenous growth factors that promote proliferation [166]. However, this possibility is not likely as exercise is associated with neuroprotection.

4.3. The Role of LINE-1 in the Neurogenic Zones

LINE-1 is typically quiescent in most somatic cell types. Its retrotransposition continues to generate both intra-individual and inter-individual genetic diversity. LINE-1

activation is strongly associated with disease development [167]. In developing neurons, LINE-1 can express and retrotranspose at a high frequency [168], but its function in mature neurons is unknown.

We used cleaved caspase-3 as a marker of middle-stage apoptosis and cleaved PARP as a marker of late apoptosis. We found both signals increased in the brain tissue at 24 hours after binge METH. METH has already been documented to have a negative impact on SVZ stem/progenitor cells, for example inducing cell death and inhibiting neurogenesis [135]. Moreover, METH self-administration was reported to cause hippocampal apoptosis at a proper dosage [134].

Our result shows that the ORF-2 signal co-localizes with some, but not all, apoptotic markers within the neurogenic zones after METH treatment. This begs the question of whether METH-induced increase of LINE-1 is in fact not associated with apoptosis. It is too early to make this conclusion. First of all, cleaved caspase-3 and cleaved PARP are the markers of caspase-dependent apoptosis. In reality, not only caspases, but also calpains [169], cathepsins [170], endonucleases, and other proteases can execute programmed cell death. Several models of caspase-independent cell death have been described. Moreover, various cell death routes may overlap and different characteristics may be displayed at the same time [171]. It is possible that a METH-induced increase of LINE-1 is associated with caspase dependent and independent cell death apoptosis. To investigate this hypothesis, we could use markers of caspase-independent apoptosis to stain brain tissue and quantify the co-localization of the markers and ORF-2. Secondly, the time point is another thing to be considered. Cadet's group found that METH treatment in immortalized rat striatal cells (M213) can caused an increase of cleavages of

caspase-3 and PARP. They also reported that initial cleavage of caspase-3 and PARP were detected at 8 hours post METH exposure. Additionally, both caspase-3 and PARP were almost completely cleaved after 16 and 24 hours post METH exposure [172]. Cadet's group showed the time course of caspase-3 activation in the striatum using Western blot analysis (pooled protein samples from 5–6 mice per group were used) [87]. They found that caspase-3 was cleaved as early as 8 hours after treatment by amphetamine (10 mg/kg, 4 times, every 2 hours). On the other hand, the appearance of TUNEL-positive cells was first seen at three days after drug administration. Both *in vivo* and *in vitro* studies indicate that our METH application model is appropriate to detect apoptosis.

Since we detected the apoptosis at 24 hours after METH injection. It is highly possible that the cells within neurogenic zones undergo apoptosis at different points of time. There are two potential solutions to fix this problem. One is adding markers for different stages of apoptosis. For example, annexin V-FITC is a common marker to specifically detect an early-to-medium stage of apoptosis while propidium iodide (PI) can detect the late stage of apoptosis. The other potential solution is to conduct some *in vitro* studies; for example, we can artificially induce cellular apoptosis and thereby ensure that all the cells undergo apoptosis at the same time. Further to that, we can quantify the co-localization between apoptosis markers and ORF-2. However, the co-localization of ORF-2 and apoptosis markers is not sufficient to conclude that a METH-induced increase of LINE-1 is associated with apoptosis. In order to study the function of LINE-1, further studies are necessary, for example, we could investigate whether suppressing or over-expressing LINE-1 could influence the level of apoptosis.

Interestingly, we found that signals of cleaved caspase-3 in the SVZ and SGZ were in the nucleus, while most papers presented cytoplasmic staining of cleaved caspase-3. To explain this, first of all, we tested our caspase-3 antibody in PC12 cells undergoing stress and we were able to obtain the image of clear cytoplasmic staining. Therefore, our antibody was deemed reliable and it was shown that METH treatment can increase cleaved caspase-3 in the nucleus in the SVZ and SGZ. In agreement with our result, there is another paper that showed cleaved caspase-3 in the nucleus [103]. In that study, the authors detected cell death in the ventricular (VZ)/SVZ of the slice culture which was from a 19-week-old human fetus after five days *in vitro* culture. It is possible that cleaved caspase-3 migrates from the cytoplasm into the nucleus 24 hours after METH exposure. In order to test the hypothesis, more *in vitro* cell studies are required to determine the time course of the migration of cleaved caspase-3 from the cytoplasm into the nucleus. Based on the literature, caspase-3 is thought to be an essential molecule involved in the nuclear morphological changes occurring in apoptotic cells. Moreover, many nuclear substrates for caspase-3 have been identified despite the cytoplasmic localization of procaspase-3. Therefore, whether cleaved caspase-3 localizes in the nucleus, and how cleaved caspase-3 has access to its nuclear targets, are important and unresolved questions. There is a study indicating that the translocation of cleaved caspase-3 from the cytoplasm into the nucleus is associated with substrate-like protein(s) during progression of apoptosis [173].

In addition to the concern of the staining pattern of cleave caspase-3, cleaved PARP staining also showed unusual pattern in the SVZ. We observed cleaved PARP staining in the cytoplasm instead of the nucleus. The previous study indicated that the PARP family is divided into three separate groups: 1) PARP1, PARPb (short PARP1), PARP2, and

PARP3, 2) PARP4 and 3) Tankyrase-1, tankyrase-2a, and its isoform tankyrase-2b (also known as PARP5 and PARP6a/b) [174]. PARP1 and 2 are considered to be nuclear enzymes and are commonly found in the nuclei of cells. In contrast, tankyrases and PARP3 are found in both the nucleus and cytoplasm [175]. At the same time, our data also showed that most of this cytoplasmic cleaved PARP staining is located at the edge of the SVZ, where the epidermal cells are.

We further checked whether METH induced increases in OFR-2 is associated with oxidative stress. We found that GSH increased at 24 hours after binge METH. Dr. Moszczynska examined the influence of binge METH (4×20 mg/kg every 5 hours) and chronic daily (20 mg/kg per day for 10 days) administration of METH on the level of total glutathione in the brain. The result suggested that binge METH treatment was associated with a regionally specific reduction of glutathione in the striatum at three hours after the last dose of METH, however, chronic METH administration did not induce a reduction of glutathione [66]. It was found that acute administration of METH (5 and 15 mg/kg) resulted in production of oxidative stress as demonstrated by decreased glutathione levels in the rat striatum and prefrontal cortex[77]. There are other studies that showed that an increased GSH level in the brain was observed in METH abusers which was thought to be a protective response to counteract the excessive oxidative stress induced by METH [78]. There is also a report that demonstrated that exposure to ionizing radiation, which can cause oxidative stress, can induce a rapid but transient decrease of the intracellular level of GSH in the brain [79]. Chronic stressors (e.g. restraint, social stress) have been associated with a significant reduction of cortical GSH or a reduction of GSH in the whole brain [176, 177]. Furthermore, it has been reported that administration of corticosterone (10 mg/kg)

significantly decreased the glutathione peroxidase (GSPx) in the hippocampus [178], and the levels of the reduced and oxidized forms of GSH in hippocampal cultures [179]. These studies further support the association between chronic stress and decreased antioxidants. Therefore, the decrease of antioxidant capacity in the brain may be responsible for the stress-related oxidative damage. As demonstrated in Chapter 1, METH can cause oxidative stress by elevating DA and GLU levels in the striatum and hippocampus [144, 180]. Increased ROS can adversely affect DNA, lipids, and cellular proteins, respectively resulting in nucleotide oxidation, lipid peroxidation or protein nitration in the striatum and hippocampus [144, 181]. The level of GSH, which plays a main role during antioxidant defense, will increase under mild oxidative stress but decrease under severe oxidative stress, such as METH administration (4×20 mg/kg) [66]. In the case of our study, we used low dosage of METH (4×10 mg/kg) and had a longer recovery time after the last injection (24h vs. 3h in the previous study), which may have led to the increased level of GSH. In conclusion, both the length of recovery time and dosage of METH affect GSH level. It is possible that chronic stress or a high dose administration of METH (4×20 mg/kg every 5 h) caused a GSH decrease due to its overutilization in the striatum, while binge METH (4×10 mg/kg, 24h) induced less oxidative stress, leading to an increased level of GSH in the hippocampus.

We also found that after METH treatment, ORF-2 co-localized with oxidative stress marker GSH in most of cells within the neurogenic zones. This result indicated that METH-induced increased LINE-1 may be associated with the responses to oxidative stress. This conclusion is supported by the previous study which reported the activation of LINE-1 induced by oxidative stress [182-184]. Wongpaiboonwattana's group found that the

methylation level of LINE-1 significantly decreased in H_2O_2-treated cells determined via PCR. This result indicated that oxidative stress can trigger LINE-1 activation [182]. Gross's group concluded that a decrease of LINE-1 methylation was associated with the increased oxidative stress in both healthy and bladder cancer subjects across the various tissue types [183]. Giorgi's group treated neuroblastoma cells with hydrogen peroxide and subjected them to an *in vitro* retrotransposition assay involving an episomal LINE-1(RP). Their results indicated that hydrogen peroxide treatment induces an increase of retrotransposition of the transiently transfected LINE-1(RP) as well as an increase of the endogenous LINE-1 transcripts. Therefore, they concluded that oxidative stress can cause LINE-1 dysregulation [184]. Kloypan's group treated bladder cancer cells (UM-UC-3 and TCCSUP) and human kidney cells (HK-2) with 20 μM H_2O_2 for 72 hours to induce oxidative stress. Their finding suggested that the ROS exposure in cells can activate glutathione synthesis via the transsulfuration pathway leading to a deficiency of Hcy. The lack of Hcy can consequently cause SAM depletion and eventual hypomethylation of LINE-1 [185]. As demonstrated in chapter 1, LINE-1 are DNA sequences which can change their position within the genome. While undergoing retrotransposition, two open reading frames transcribe to RNA and translate to ORF-1 and ORF-2 proteins. These two proteins perform LINE-1 retrotransposition [98-101]. In addition to this function, ORF-1 protein is distinctive in forming large cytoplasmic foci, which are identified as cytoplasmic stress granules (LINE-1 ORF1 Protein Localizes in Stress Granules with Other RNA-Binding Proteins, Including Components of RNA Interference RNA-Induced Silencing Complex). The function of stress granules includes protection of RNA from harmful conditions, thus their appearance under stress is a protective response [186]. That could

potentially be the reason why we observe increased co-localization between ORF-2 and GSH after METH administration.

One topic necessary for future consideration is whether GSH is the appropriate marker to test oxidative stress. As demonstrated in Chapter 1, total GSH exists as free form or bound to proteinsin cells. The relationship between GSH and ROS is a dynamic balance process that underpins reduction/oxidation (redox) regulation and signaling. Since glutathione reductase, which can revert free glutathione from its oxidized form (GSSG), is constitutively active and inducible upon oxidative stress, free glutathione exists almost exclusively in its reduced form. The ratio of reduced to oxidized glutathione within cells is often used as a marker of oxidative stress [187-190]. To test the relationship between oxidative stress and increased LINE-1 after METH administration, a study to determine the ratio of GSH to GSSG is necessary. Moreover, the suppression or overexpression of LINE-1 in the cells or animal could serve as models to investigate this relationship.

In summary, we have determined that OFR-2 increased in mature neurons and GFAP-positive cells after METH treatment. To determine whether binge METH induced upregulation of ORF-2 in mature neurons and glia, triple staining study for ORF-2, GSH:GSSG and GFAP (or NeuN) may be required.

4.4. Interpretation of the co-localization results

We used the Pearson correlation coefficient (PCC) to determine the correlation of two fluorescence channels and consequently determine the co-localization of signals from the two channels [191]. This is a well-established method to determine correlation, and has a range of +1 (perfect correlation) to −1 (perfect but negative correlation) with 0

denoting the absence of a relationship. Its application to the measurement of co-localization between fluorophores is relatively recent [192]. The PCC also has some drawbacks. It is not sensitive to differences in signal intensity between the components of an image caused by different labeling with fluorochromes, photobleaching, or different settings of amplifiers, and the negative values of the correlation coefficient are difficult to interpret when the degree of overlap is the quantity to be measured [191]. In our case, OFR-2 showed cytoplasmic staining while NeuN, Ki-67, and cleaved PARP staining were located in the nucleus. The PCC cannot paint the whole picture because the two stainings in which we are interested (e.g. ORF2/NeuN, ORF2/Ki-67) do not actually co-occur. Stereology-based counting of cells co-expressing two fluorophores in different cellular compartments is warranted.

4.5. Conclusions and Future Directions

Our results suggest that systemic administration of neurotoxic doses of binge METH increases the activity of LINE-1 in GFAP-positive cells and postmitotic neuronal cells as well as in cells with increased GSH in the neurogenic zones. Binge METH can induce increased activity of LINE-1 in the neurogenic zones which may not be associated with apoptotic cell death but may be associated with responses to oxidative stress.

As mentioned before, we exclusively evaluated the apoptosis status at 24 hours after METH injection. It is highly possible that the cells within neurogenic zones undergo apoptosis at different time points, therefore, to better investigate the apoptosis status of cells after METH treatment, a *in vivo* time course is required. In future, to determine the relation between LINE1 and METH induced apoptosis, different apoptotic markers (e.g.

annexinV-FITC) should be used. In addition, a time course study in PC12 cells after the exposure of METH should be conducted to study the relationship between METH-induced apoptosis and the activation and nucleus translocation of cleaved caspase-3. Moreover, a study to determine the ratio of GSH:GSSG in the zones of interest after binge METH will be valuable. Last but not least, studies to investigate the functional link between LINE-1 and oxidative stress in METH neurotoxicity and to determine LINE-1 function in glial cells would be worth performing and would help to explain our results.

REFERENCES

1. Anglin, M.D., et al., History of the methamphetamine problem. J Psychoactive Drugs, 2000. 32(2): p. 137-41.
2. Vearrier, D., et al., Methamphetamine: history, pathophysiology, adverse health effects, current trends, and hazards associated with the clandestine manufacture of methamphetamine. Dis Mon, 2012. 58(2): p. 38-89.
3. Gonzales, R., L. Mooney, and R.A. Rawson, The methamphetamine problem in the United States. Annu Rev Public Health, 2010. 31: p. 385-98.
4. Derlet, R.W. and B. Heischober, Methamphetamine. Stimulant of the 1990s? West J Med, 1990. 153(6): p. 625-8.
5. Shin, E.J., et al., Current understanding of methamphetamine-associated dopaminergic neurodegeneration and psychotoxic behaviors. Arch Pharm Res, 2017. 40(4): p. 403-428.
6. Chomchai, C. and S. Chomchai, Global patterns of methamphetamine use. Curr Opin Psychiatry, 2015. 28(4): p. 269-74.
7. Meng, Y., et al., Pharmacological effects of methamphetamine and other stimulants via inhalation exposure. Drug Alcohol Depend, 1999. 53(2): p. 111-20.
8. Klasser, G.D. and J. Epstein, Methamphetamine and its impact on dental care. J Can Dent Assoc, 2005. 71(10): p. 759-62.
9. Albertson, T.E., R.W. Derlet, and B.E. Van Hoozen, Methamphetamine and the expanding complications of amphetamines. West J Med, 1999. 170(4): p. 214-9.
10. Sulzer, D., et al., Mechanisms of neurotransmitter release by amphetamines: a review. Prog Neurobiol, 2005. 75(6): p. 406-33.

11. Murray, J.B., Psychophysiological aspects of amphetamine-methamphetamine abuse. J Psychol, 1998. 132(2): p. 227-37.

12. Saltman, D.C., et al., Experiences in managing problematic crystal methamphetamine use and associated depression in gay men and HIV positive men: in-depth interviews with general practitioners in Sydney, Australia. BMC Fam Pract, 2008. 9: p. 45.

13. Volkow, N.D., et al., Association of dopamine transporter reduction with psychomotor impairment in methamphetamine abusers. Am J Psychiatry, 2001. 158(3): p. 377-82.

14. Lambert, N.M., et al., Hyperactive children and the efficacy of psychoactive drugs as a treatment intervention. Am J Orthopsychiatry, 1976. 46(2): p. 335-52.

15. Rolls, E.T., Limbic systems for emotion and for memory, but no single limbic system. Cortex, 2015. 62: p. 119-57.

16. Smith, K.S. and K.C. Berridge, Opioid limbic circuit for reward: interaction between hedonic hotspots of nucleus accumbens and ventral pallidum. J Neurosci, 2007. 27(7): p. 1594-605.

17. Vollm, B.A., et al., Methamphetamine activates reward circuitry in drug naive human subjects. Neuropsychopharmacology, 2004. 29(9): p. 1715-22.

18. Bowyer, J.F., et al., Further studies of the role of hyperthermia in methamphetamine neurotoxicity. J Pharmacol Exp Ther, 1994. 268(3): p. 1571-80.

19. Ali, S.F., et al., Low environmental temperatures or pharmacologic agents that produce hypothermia decrease methamphetamine neurotoxicity in mice. Brain Res, 1994. 658(1-2): p. 33-8.

20. Yamamoto, B.K., A. Moszczynska, and G.A. Gudelsky, Amphetamine toxicities: classical and emerging mechanisms. Ann N Y Acad Sci, 2010. 1187: p. 101-21.

21. Bowyer, J.F., The role of hyperthermia in amphetamine's interactions with NMDA receptors, nitric oxide, and age to produce neurotoxicity. Ann N Y Acad Sci, 1995. 765: p. 309-10.

22. Ali, S.F., G.D. Newport, and W. Slikker, Jr., Methamphetamine-induced dopaminergic toxicity in mice. Role of environmental temperature and pharmacological agents. Ann N Y Acad Sci, 1996. 801: p. 187-98.

23. Fleckenstein, A.E., et al., Interaction between hyperthermia and oxygen radical formation in the 5-hydroxytryptaminergic response to a single methamphetamine administration. J Pharmacol Exp Ther, 1997. 283(1): p. 281-5.

24. Rothman, R.B. and M.H. Baumann, Monoamine transporters and psychostimulant drugs. Eur J Pharmacol, 2003. 479(1-3): p. 23-40.

25. Fleckenstein, A.E., et al., New insights into the mechanism of action of amphetamines. Annu Rev Pharmacol Toxicol, 2007. 47: p. 681-98.

26. Sulzer, D. and S. Rayport, Amphetamine and other psychostimulants reduce pH gradients in midbrain dopaminergic neurons and chromaffin granules: a mechanism of action. Neuron, 1990. 5(6): p. 797-808.

27. Brown, J.M., et al., A single methamphetamine administration rapidly decreases vesicular dopamine uptake. J Pharmacol Exp Ther, 2002. 302(2): p. 497-501.

28. Hansen, J.P., et al., Methylenedioxymethamphetamine decreases plasmalemmal and vesicular dopamine transport: mechanisms and implications for neurotoxicity. J Pharmacol Exp Ther, 2002. 300(3): p. 1093-100.

29. Sulzer, D., et al., Amphetamine redistributes dopamine from synaptic vesicles to the cytosol and promotes reverse transport. J Neurosci, 1995. 15(5 Pt 2): p. 4102-8.

30. Fleckenstein, A.E., et al., A rapid and reversible change in dopamine transporters induced by methamphetamine. Eur J Pharmacol, 1997. 323(2-3): p. R9-10.

31. Mark, K.A., J.J. Soghomonian, and B.K. Yamamoto, High-dose methamphetamine acutely activates the striatonigral pathway to increase striatal glutamate and mediate long-term dopamine toxicity. J Neurosci, 2004. 24(50): p. 11449-56.

32. Ricaurte, G.A., C.R. Schuster, and L.S. Seiden, Long-term effects of repeated methylamphetamine administration on dopamine and serotonin neurons in the rat brain: a regional study. Brain Res, 1980. 193(1): p. 153-63.

33. Wagner, G.C., et al., Long-lasting depletions of striatal dopamine and loss of dopamine uptake sites following repeated administration of methamphetamine. Brain Res, 1980. 181(1): p. 151-60.

34. Seiden, L.S., et al., Neurotoxicity in dopamine and 5-hydroxytryptamine terminal fields: a regional analysis in nigrostriatal and mesolimbic projections. Ann N Y Acad Sci, 1988. 537: p. 161-72.

35. Woolverton, W.L., et al., Long-term effects of chronic methamphetamine administration in rhesus monkeys. Brain Res, 1989. 486(1): p. 73-8.

36. Hotchkiss, A.J. and J.W. Gibb, Long-term effects of multiple doses of methamphetamine on tryptophan hydroxylase and tyrosine hydroxylase activity in rat brain. J Pharmacol Exp Ther, 1980. 214(2): p. 257-62.

37. Lorez, H., Fluorescence histochemistry indicates damage of striatal dopamine nerve terminals in rats after multiple doses of methamphetamine. Life Sci, 1981. 28(8): p. 911-6.

38. Sharma, H.S. and E.A. Kiyatkin, Rapid morphological brain abnormalities during acute methamphetamine intoxication in the rat: an experimental study using light and electron microscopy. J Chem Neuroanat, 2009. 37(1): p. 18-32.

39. Rusyniak, D.E., Neurologic manifestations of chronic methamphetamine abuse. Psychiatr Clin North Am, 2013. 36(2): p. 261-75.

40. Wilson, J.M., et al., Striatal dopamine nerve terminal markers in human, chronic methamphetamine users. Nat Med, 1996. 2(6): p. 699-703.

41. Sekine, Y., et al., Brain serotonin transporter density and aggression in abstinent methamphetamine abusers. Arch Gen Psychiatry, 2006. 63(1): p. 90-100.

42. Cadet, J.L., S. Jayanthi, and X. Deng, Methamphetamine-induced neuronal apoptosis involves the activation of multiple death pathways. Review. Neurotox Res, 2005. 8(3-4): p. 199-206.

43. Kadota, T. and K. Kadota, Neurotoxic morphological changes induced in the medial prefrontal cortex of rats behaviorally sensitized to methamphetamine. Arch Histol Cytol, 2004. 67(3): p. 241-51.

44. Marshall, J.F. and S.J. O'Dell, Methamphetamine influences on brain and behavior: unsafe at any speed? Trends Neurosci, 2012. 35(9): p. 536-45.

45. Kuczenski, R., et al., Escalating dose-multiple binge methamphetamine exposure results in degeneration of the neocortex and limbic system in the rat. Exp Neurol, 2007. 207(1): p. 42-51.

46. Deng, X., et al., Methamphetamine causes widespread apoptosis in the mouse brain: evidence from using an improved TUNEL histochemical method. Brain Res Mol Brain Res, 2001. 93(1): p. 64-9.

47. Zhu, J.P., W. Xu, and J.A. Angulo, Methamphetamine-induced cell death: selective vulnerability in neuronal subpopulations of the striatum in mice. Neuroscience, 2006. 140(2): p. 607-22.

48. Tokunaga, I., et al., The peroxidative DNA damage and apoptosis in methamphetamine-treated rat brain. J Med Invest, 2008. 55(3-4): p. 241-5.

49. Kitamura, O., et al., Immunohistochemical investigation of dopaminergic terminal markers and caspase-3 activation in the striatum of human methamphetamine users. Int J Legal Med, 2007. 121(3): p. 163-8.

50. Jayanthi, S., et al., Methamphetamine causes differential regulation of pro-death and anti-death Bcl-2 genes in the mouse neocortex. FASEB J, 2001. 15(10): p. 1745-52.

51. Jayanthi, S., et al., Calcineurin/NFAT-induced up-regulation of the Fas ligand/Fas death pathway is involved in methamphetamine-induced neuronal apoptosis. Proc Natl Acad Sci U S A, 2005. 102(3): p. 868-73.

52. Guilarte, T.R., et al., Methamphetamine-induced deficits of brain monoaminergic neuronal markers: distal axotomy or neuronal plasticity. Neuroscience, 2003. 122(2): p. 499-513.

53. Thomas, D.M., et al., Methamphetamine neurotoxicity in dopamine nerve endings of the striatum is associated with microglial activation. J Pharmacol Exp Ther, 2004. 311(1): p. 1-7.

54. Fantegrossi, W.E., et al., A comparison of the physiological, behavioral, neurochemical and microglial effects of methamphetamine and 3,4-methylenedioxymethamphetamine in the mouse. Neuroscience, 2008. 151(2): p. 533-43.

55. Pubill, D., et al., Different glial response to methamphetamine- and methylenedioxymethamphetamine-induced neurotoxicity. Naunyn Schmiedebergs Arch Pharmacol, 2003. 367(5): p. 490-9.

56. Escubedo, E., et al., Microgliosis and down-regulation of adenosine transporter induced by methamphetamine in rats. Brain Res, 1998. 814(1-2): p. 120-6.

57. Pu, C. and C.V. Vorhees, Developmental dissociation of methamphetamine-induced depletion of dopaminergic terminals and astrocyte reaction in rat striatum. Brain Res Dev Brain Res, 1993. 72(2): p. 325-8.

58. Carmena, A., et al., Methamphetamine-induced toxicity in indusium griseum of mice is associated with astro- and microgliosis. Neurotox Res, 2015. 27(3): p. 209-16.

59. Thomas, D.M. and D.M. Kuhn, Cyclooxygenase-2 is an obligatory factor in methamphetamine-induced neurotoxicity. J Pharmacol Exp Ther, 2005. 313(2): p. 870-6.

60. Nash, J.F. and B.K. Yamamoto, Methamphetamine neurotoxicity and striatal glutamate release: comparison to 3,4-methylenedioxymethamphetamine. Brain Res, 1992. 581(2): p. 237-43.

61. Vicente-Rodriguez, M., et al., Pleiotrophin overexpression regulates amphetamine-induced reward and striatal dopaminergic denervation without changing the

expression of dopamine D1 and D2 receptors: Implications for neuroinflammation. Eur Neuropsychopharmacol, 2016. 26(11): p. 1794-1805.

62. Cubells, J.F., et al., Methamphetamine neurotoxicity involves vacuolation of endocytic organelles and dopamine-dependent intracellular oxidative stress. J Neurosci, 1994. 14(4): p. 2260-71.

63. Graham, D.G., Oxidative pathways for catecholamines in the genesis of neuromelanin and cytotoxic quinones. Mol Pharmacol, 1978. 14(4): p. 633-43.

64. Esteves, A.R., et al., Mitochondrial function in Parkinson's disease cybrids containing an nt2 neuron-like nuclear background. Mitochondrion, 2008. 8(3): p. 219-28.

65. Imam, S.Z., et al., Prevention of dopaminergic neurotoxicity by targeting nitric oxide and peroxynitrite: implications for the prevention of methamphetamine-induced neurotoxic damage. Ann N Y Acad Sci, 2000. 914: p. 157-71.

66. Moszczynska, A., S. Turenne, and S.J. Kish, Rat striatal levels of the antioxidant glutathione are decreased following binge administration of methamphetamine. Neurosci Lett, 1998. 255(1): p. 49-52.

67. Jayanthi, S., B. Ladenheim, and J.L. Cadet, Methamphetamine-induced changes in antioxidant enzymes and lipid peroxidation in copper/zinc-superoxide dismutase transgenic mice. Ann N Y Acad Sci, 1998. 844: p. 92-102.

68. D'Almeida, V., et al., Antioxidant defense in rat brain after chronic treatment with anorectic drugs. Toxicol Lett, 1995. 81(2-3): p. 101-5.

69. Fukami, G., et al., Effect of antioxidant N-acetyl-L-cysteine on behavioral changes and neurotoxicity in rats after administration of methamphetamine. Brain Res, 2004. 1016(1): p. 90-5.

70. Kuribayashi, K., P.A. Mayes, and W.S. El-Deiry, What are caspases 3 and 7 doing upstream of the mitochondria? Cancer Biol Ther, 2006. 5(7): p. 763-5.

71. Lakhani, S.A., et al., Caspases 3 and 7: key mediators of mitochondrial events of apoptosis. Science, 2006. 311(5762): p. 847-51.

72. Gagne, J.P., et al., Proteomic investigation of phosphorylation sites in poly(ADP-ribose) polymerase-1 and poly(ADP-ribose) glycohydrolase. J Proteome Res, 2009. 8(2): p. 1014-29.

73. Mathieu, J., et al., A PARP-1/JNK1 cascade participates in the synergistic apoptotic effect of TNFalpha and all-trans retinoic acid in APL cells. Oncogene, 2008. 27(24): p. 3361-70.

74. Heeres, J.T. and P.J. Hergenrother, Poly(ADP-ribose) makes a date with death. Curr Opin Chem Biol, 2007. 11(6): p. 644-53.

75. Agarwal, A., et al., Potential biological role of poly (ADP-ribose) polymerase (PARP) in male gametes. Reprod Biol Endocrinol, 2009. 7: p. 143.

76. Aoyama, K., M. Watabe, and T. Nakaki, Regulation of neuronal glutathione synthesis. J Pharmacol Sci, 2008. 108(3): p. 227-38.

77. Acikgoz, O., et al., Methamphetamine causes depletion of glutathione and an increase in oxidized glutathione in the rat striatum and prefrontal cortex. Neurotox Res, 2001. 3(3): p. 277-80.

78. Huang, M.C., et al., Oxidative stress status in recently abstinent methamphetamine abusers. Psychiatry Clin Neurosci, 2013. 67(2): p. 92-100.

79. Davidson, C., et al., Methamphetamine neurotoxicity: necrotic and apoptotic mechanisms and relevance to human abuse and treatment. Brain Res Brain Res Rev, 2001. 36(1): p. 1-22.

80. Krasnova, I.N. and J.L. Cadet, Methamphetamine toxicity and messengers of death. Brain Res Rev, 2009. 60(2): p. 379-407.

81. Seiden, L.S. and K.E. Sabol, Methamphetamine and methylenedioxymethamphetamine neurotoxicity: possible mechanisms of cell destruction. NIDA Res Monogr, 1996. 163: p. 251-76.

82. LaGasse, L.L., et al., Prenatal methamphetamine exposure and childhood behavior problems at 3 and 5 years of age. Pediatrics, 2012. 129(4): p. 681-8.

83. Volkow, N.D., et al., Loss of dopamine transporters in methamphetamine abusers recovers with protracted abstinence. J Neurosci, 2001. 21(23): p. 9414-8.

84. Baptista, S., et al., Methamphetamine decreases dentate gyrus stem cell self-renewal and shifts the differentiation towards neuronal fate. Stem Cell Res, 2014. 13(2): p. 329-41.

85. Kish, S.J., et al., Brain dopamine neurone 'damage': methamphetamine users vs. Parkinson's disease - a critical assessment of the evidence. Eur J Neurosci, 2017. 45(1): p. 58-66.

86. Moszczynska, A., et al., Neurotoxic Methamphetamine Doses Increase LINE-1 Expression in the Neurogenic Zones of the Adult Rat Brain. Sci Rep, 2015. 5: p. 14356.

87. Cadet, J.L., et al., Transcriptional and epigenetic substrates of methamphetamine addiction and withdrawal: evidence from a long-access self-administration model in the rat. Mol Neurobiol, 2015. 51(2): p. 696-717.

88. Omonijo, O., et al., Differential effects of binge methamphetamine injections on the mRNA expression of histone deacetylases (HDACs) in the rat striatum. Neurotoxicology, 2014. 45: p. 178-84.

89. Jiang, W., et al., Epigenetic upregulation of alpha-synuclein in the rats exposed to methamphetamine. Eur J Pharmacol, 2014. 745: p. 243-8.

90. Hata, K. and Y. Sakaki, Identification of critical CpG sites for repression of L1 transcription by DNA methylation. Gene, 1997. 189(2): p. 227-34.

91. Bennetzen, J.L., Transposable element contributions to plant gene and genome evolution. Plant Mol Biol, 2000. 42(1): p. 251-69.

92. Bannert, N. and R. Kurth, Retroelements and the human genome: new perspectives on an old relation. Proc Natl Acad Sci U S A, 2004. 101 Suppl 2: p. 14572-9.

93. Goodier, J.L. and H.H. Kazazian, Jr., Retrotransposons revisited: the restraint and rehabilitation of parasites. Cell, 2008. 135(1): p. 23-35.

94. Brouha, B., et al., Hot L1s account for the bulk of retrotransposition in the human population. Proc Natl Acad Sci U S A, 2003. 100(9): p. 5280-5.

95. Cost, G.J., et al., Human L1 element target-primed reverse transcription in vitro. EMBO J, 2002. 21(21): p. 5899-910.

96. Kazazian, H.H., Jr. and J.L. Goodier, LINE drive. retrotransposition and genome instability. Cell, 2002. 110(3): p. 277-80.

97. Babushok, D.V. and H.H. Kazazian, Jr., Progress in understanding the biology of the human mutagen LINE-1. Hum Mutat, 2007. 28(6): p. 527-39.

98. Hohjoh, H. and M.F. Singer, Cytoplasmic ribonucleoprotein complexes containing human LINE-1 protein and RNA. EMBO J, 1996. 15(3): p. 630-9.

99. Goodier, J.L., et al., LINE-1 ORF1 protein localizes in stress granules with other RNA-binding proteins, including components of RNA interference RNA-induced silencing complex. Mol Cell Biol, 2007. 27(18): p. 6469-83.

100. Mathias, S.L., et al., Reverse transcriptase encoded by a human transposable element. Science, 1991. 254(5039): p. 1808-10.

101. Feng, Q., et al., Human L1 retrotransposon encodes a conserved endonuclease required for retrotransposition. Cell, 1996. 87(5): p. 905-16.

102. Gasior, S.L., et al., The human LINE-1 retrotransposon creates DNA double-strand breaks. J Mol Biol, 2006. 357(5): p. 1383-93.

103. Coufal, N.G., et al., L1 retrotransposition in human neural progenitor cells. Nature, 2009. 460(7259): p. 1127-31.

104. Baillie, J.K., et al., Somatic retrotransposition alters the genetic landscape of the human brain. Nature, 2011. 479(7374): p. 534-7.

105. Gilbert, N., S. Lutz-Prigge, and J.V. Moran, Genomic deletions created upon LINE-1 retrotransposition. Cell, 2002. 110(3): p. 315-25.

106. Haoudi, A., et al., Retrotransposition-Competent Human LINE-1 Induces Apoptosis in Cancer Cells With Intact p53. J Biomed Biotechnol, 2004. 2004(4): p. 185-194.

107. Stetson, D.B., et al., Trex1 prevents cell-intrinsic initiation of autoimmunity. Cell, 2008. 134(4): p. 587-98.

108. Okudaira, N., Y. Ishizaka, and H. Nishio, Retrotransposition of long interspersed element 1 induced by methamphetamine or cocaine. J Biol Chem, 2014. 289(37): p. 25476-85.

109. Gross, C.G., Neurogenesis in the adult brain: death of a dogma. Nat Rev Neurosci, 2000. 1(1): p. 67-73.

110. Cameron, H.A. and R.D. McKay, Adult neurogenesis produces a large pool of new granule cells in the dentate gyrus. J Comp Neurol, 2001. 435(4): p. 406-17.

111. Ming, G.L. and H. Song, Adult neurogenesis in the mammalian central nervous system. Annu Rev Neurosci, 2005. 28: p. 223-50.

112. Ma, D.K., et al., Adult neural stem cells in the mammalian central nervous system. Cell Res, 2009. 19(6): p. 672-82.

113. Alvarez-Buylla, A. and D.A. Lim, For the long run: maintaining germinal niches in the adult brain. Neuron, 2004. 41(5): p. 683-6.

114. Duan, X., et al., Development of neural stem cell in the adult brain. Curr Opin Neurobiol, 2008. 18(1): p. 108-15.

115. Eriksson, P.S., et al., Neurogenesis in the adult human hippocampus. Nat Med, 1998. 4(11): p. 1313-7.

116. Kempermann, G., L. Wiskott, and F.H. Gage, Functional significance of adult neurogenesis. Curr Opin Neurobiol, 2004. 14(2): p. 186-91.

117. Zhao, C., W. Deng, and F.H. Gage, Mechanisms and functional implications of adult neurogenesis. Cell, 2008. 132(4): p. 645-60.

118. Yan, Y.P., et al., Persistent migration of neuroblasts from the subventricular zone to the injured striatum mediated by osteopontin following intracerebral hemorrhage. J Neurochem, 2009. 109(6): p. 1624-35.

119. Markakis, E.A. and F.H. Gage, Adult-generated neurons in the dentate gyrus send axonal projections to field CA3 and are surrounded by synaptic vesicles. J Comp Neurol, 1999. 406(4): p. 449-60.

120. Steiner, B., et al., Type-2 cells as link between glial and neuronal lineage in adult hippocampal neurogenesis. Glia, 2006. 54(8): p. 805-14.

121. Seri, B., et al., Astrocytes give rise to new neurons in the adult mammalian hippocampus. J Neurosci, 2001. 21(18): p. 7153-60.

122. van Praag, H., et al., Functional neurogenesis in the adult hippocampus. Nature, 2002. 415(6875): p. 1030-4.

123. Luskin, M.B., Restricted proliferation and migration of postnatally generated neurons derived from the forebrain subventricular zone. Neuron, 1993. 11(1): p. 173-89.

124. Peterson, D.A., Stem cells in brain plasticity and repair. Curr Opin Pharmacol, 2002. 2(1): p. 34-42.

125. Abrous, D.N., M. Koehl, and M. Le Moal, Adult neurogenesis: from precursors to network and physiology. Physiol Rev, 2005. 85(2): p. 523-69.

126. Falconer, E.M. and L.A. Galea, Sex differences in cell proliferation, cell death and defensive behavior following acute predator odor stress in adult rats. Brain Res, 2003. 975(1-2): p. 22-36.

127. Kee, N., et al., The utility of Ki-67 and BrdU as proliferative markers of adult neurogenesis. J Neurosci Methods, 2002. 115(1): p. 97-105.

128. Francis, F., et al., Doublecortin is a developmentally regulated, microtubule-associated protein expressed in migrating and differentiating neurons. Neuron, 1999. 23(2): p. 247-56.

129. Mullen, R.J., C.R. Buck, and A.M. Smith, NeuN, a neuronal specific nuclear protein in vertebrates. Development, 1992. 116(1): p. 201-11.

130. Thompson, P.M., et al., Structural abnormalities in the brains of human subjects who use methamphetamine. J Neurosci, 2004. 24(26): p. 6028-36.

131. Altman, J. and G.D. Das, Autoradiographic and histological evidence of postnatal hippocampal neurogenesis in rats. J Comp Neurol, 1965. 124(3): p. 319-35.

132. Yamashima, T., A.B. Tonchev, and M. Yukie, Adult hippocampal neurogenesis in rodents and primates: endogenous, enhanced, and engrafted. Rev Neurosci, 2007. 18(1): p. 67-82.

133. Hori, N., et al., Neurotoxic effects of methamphetamine on rat hippocampus pyramidal neurons. Cell Mol Neurobiol, 2010. 30(6): p. 849-56.

134. Mandyam, C.D., et al., Varied access to intravenous methamphetamine self-administration differentially alters adult hippocampal neurogenesis. Biol Psychiatry, 2008. 64(11): p. 958-65.

135. Bento, A.R., et al., Methamphetamine exerts toxic effects on subventricular zone stem/progenitor cells and inhibits neuronal differentiation. Rejuvenation Res, 2011. 14(2): p. 205-14.

136. Eyerman, D.J. and B.K. Yamamoto, A rapid oxidation and persistent decrease in the vesicular monoamine transporter 2 after methamphetamine. J Neurochem, 2007. 103(3): p. 1219-27.

137. Halpin, L.E., S.A. Collins, and B.K. Yamamoto, Neurotoxicity of methamphetamine and 3,4-methylenedioxymethamphetamine. Life Sci, 2014. 97(1): p. 37-44.

138. Spadafora, C., A LINE-1-encoded reverse transcriptase-dependent regulatory mechanism is active in embryogenesis and tumorigenesis. Ann N Y Acad Sci, 2015. 1341: p. 164-71.

139. Vitullo, P., et al., LINE-1 retrotransposon copies are amplified during murine early embryo development. Mol Reprod Dev, 2012. 79(2): p. 118-27.

140. Ostertag, E.M., et al., A mouse model of human L1 retrotransposition. Nat Genet, 2002. 32(4): p. 655-60.

141. Muotri, A.R., et al., Somatic mosaicism in neuronal precursor cells mediated by L1 retrotransposition. Nature, 2005. 435(7044): p. 903-10.

142. Teneng, I., V. Stribinskis, and K.S. Ramos, Context-specific regulation of LINE-1. Genes Cells, 2007. 12(10): p. 1101-10.

143. Stribinskis, V. and K.S. Ramos, Activation of human long interspersed nuclear element 1 retrotransposition by benzo(a)pyrene, an ubiquitous environmental carcinogen. Cancer Res, 2006. 66(5): p. 2616-20.

144. Yamamoto, B.K. and W. Zhu, The effects of methamphetamine on the production of free radicals and oxidative stress. J Pharmacol Exp Ther, 1998. 287(1): p. 107-14.

145. Venkatesan, A., et al., Impairment of adult hippocampal neural progenitor proliferation by methamphetamine: role for nitrotyrosination. Mol Brain, 2011. 4: p. 28.

146. Ekthuwapranee, K., A. Sotthibundhu, and P. Govitrapong, Melatonin attenuates methamphetamine-induced inhibition of proliferation of adult rat hippocampal progenitor cells in vitro. J Pineal Res, 2015. 58(4): p. 418-28.

147. Mao, L. and J.Q. Wang, Gliogenesis in the striatum of the adult rat: alteration in neural progenitor population after psychostimulant exposure. Brain Res Dev Brain Res, 2001. 130(1): p. 41-51.

148. Teuchert-Noodt, G., R.R. Dawirs, and K. Hildebrandt, Adult treatment with methamphetamine transiently decreases dentate granule cell proliferation in the gerbil hippocampus. J Neural Transm (Vienna), 2000. 107(2): p. 133-43.

149. Kim, A. and C.D. Mandyam, Methamphetamine affects cell proliferation in the medial prefrontal cortex: a new niche for toxicity. Pharmacology, biochemistry, and behavior, 2014. 126: p. 90-96.

150. Mandyam, C.D., et al., Varied access to intravenous methamphetamine self-administration differentially alters adult hippocampal neurogenesis. Biological psychiatry, 2008. 64(11): p. 958-965.

151. Banaz-Yasar, F., et al., LINE-1 retrotransposition events affect endothelial proliferation and migration. Histochem Cell Biol, 2010. 134(6): p. 581-9.

152. Li, M.Y., et al., Long interspersed nucleotide acid element-1 ORF-1 protein promotes proliferation and invasion of human colorectal cancer LoVo cells through enhancing ETS-1 activity. Genet Mol Res, 2014. 13(3): p. 6981-94.

153. Macia, A., et al., Engineered LINE-1 retrotransposition in nondividing human neurons. Genome Res, 2017. 27(3): p. 335-348.

154. Carleton, A., et al., Becoming a new neuron in the adult olfactory bulb. Nat Neurosci, 2003. 6(5): p. 507-18.

155. Abekawa, T., et al., Developmental GABAergic deficit enhances methamphetamine-induced apoptosis. Psychopharmacology (Berl), 2011. 215(3): p. 413-27.

156. Li, Y., et al., Taurine attenuates methamphetamine-induced autophagy and apoptosis in PC12 cells through mTOR signaling pathway. Toxicol Lett, 2012. 215(1): p. 1-7.

157. Qiao, D., et al., Insulin-like growth factor binding protein 5 (IGFBP5) mediates methamphetamine-induced dopaminergic neuron apoptosis. Toxicol Lett, 2014. 230(3): p. 444-53.

158. Kempermann, G., et al., Milestones of neuronal development in the adult hippocampus. Trends Neurosci, 2004. 27(8): p. 447-52.

159. Kempermann, G., H. Song, and F.H. Gage, Neurogenesis in the Adult Hippocampus. Cold Spring Harb Perspect Biol, 2015. 7(9): p. a018812.

160. Raineri, M., et al., Differential effects of environment-induced changes in body temperature on modafinil's actions against methamphetamine-induced striatal toxicity in mice. Neurotox Res, 2015. 27(1): p. 71-83.

161. Muotri, A.R., L1 Retrotransposition in Neural Progenitor Cells. Methods Mol Biol, 2016. 1400: p. 157-63.

162. Upton, K.R., et al., Ubiquitous L1 mosaicism in hippocampal neurons. Cell, 2015. 161(2): p. 228-39.

163. Wang, D.D. and A. Bordey, The astrocyte odyssey. Prog Neurobiol, 2008. 86(4): p. 342-67.

164. Mandyam, C.D., et al., Methamphetamine self-administration and voluntary exercise have opposing effects on medial prefrontal cortex gliogenesis. J Neurosci, 2007. 27(42): p. 11442-50.

165. Van Kampen, J.M., T. Hagg, and H.A. Robertson, Induction of neurogenesis in the adult rat subventricular zone and neostriatum following dopamine D3 receptor stimulation. Eur J Neurosci, 2004. 19(9): p. 2377-87.

166. Olson, A.K., et al., Environmental enrichment and voluntary exercise massively increase neurogenesis in the adult hippocampus via dissociable pathways. Hippocampus, 2006. 16(3): p. 250-60.

167. Richardson, S.R., et al., The Influence of LINE-1 and SINE Retrotransposons on Mammalian Genomes. Microbiol Spectr, 2015. 3(2): p. MDNA3-0061-2014.

168. Thomas, C.A., A.C. Paquola, and A.R. Muotri, LINE-1 retrotransposition in the nervous system. Annu Rev Cell Dev Biol, 2012. 28: p. 555-73.

169. Broker, L.E., et al., Cathepsin B mediates caspase-independent cell death induced by microtubule stabilizing agents in non-small cell lung cancer cells. Cancer Res, 2004. 64(1): p. 27-30.

170. Yamashima, T., et al., Inhibition of ischaemic hippocampal neuronal death in primates with cathepsin B inhibitor CA-074: a novel strategy for neuroprotection based on 'calpain-cathepsin hypothesis'. Eur J Neurosci, 1998. 10(5): p. 1723-33.

171. Broker, L.E., F.A. Kruyt, and G. Giaccone, Cell death independent of caspases: a review. Clin Cancer Res, 2005. 11(9): p. 3155-62.

172. Deng, X., et al., Methamphetamine induces apoptosis in an immortalized rat striatal cell line by activating the mitochondrial cell death pathway. Neuropharmacology, 2002. 42(6): p. 837-45.

173. Resendes, A.R., et al., Apoptosis in normal lymphoid organs from healthy normal, conventional pigs at different ages detected by TUNEL and cleaved caspase-3 immunohistochemistry in paraffin-embedded tissues. Vet Immunol Immunopathol, 2004. 99(3-4): p. 203-13.

174. Hassa, P.O. and M.O. Hottiger, The diverse biological roles of mammalian PARPS, a small but powerful family of poly-ADP-ribose polymerases. Front Biosci, 2008. 13: p. 3046-82.

175. Augustin, A., et al., PARP-3 localizes preferentially to the daughter centriole and interferes with the G1/S cell cycle progression. J Cell Sci, 2003. 116(Pt 8): p. 1551-62.

176. Madrigal, J.L., et al., Glutathione depletion, lipid peroxidation and mitochondrial dysfunction are induced by chronic stress in rat brain. Neuropsychopharmacology, 2001. 24(4): p. 420-9.

177. Huong, N.T., et al., Social isolation stress-induced oxidative damage in mouse brain and its modulation by majonoside-R2, a Vietnamese ginseng saponin. Biol Pharm Bull, 2005. 28(8): p. 1389-93.

178. McIntosh, L.J., K.E. Hong, and R.M. Sapolsky, Glucocorticoids may alter antioxidant enzyme capacity in the brain: baseline studies. Brain Res, 1998. 791(1-2): p. 209-14.

179. Patel, R., et al., Disruptive effects of glucocorticoids on glutathione peroxidase biochemistry in hippocampal cultures. J Neurochem, 2002. 82(1): p. 118-25.

180. Giovanni, A., et al., Estimating hydroxyl radical content in rat brain using systemic and intraventricular salicylate: impact of methamphetamine. J Neurochem, 1995. 64(4): p. 1819-25.

181. Acikgoz, O., et al., Methamphetamine causes lipid peroxidation and an increase in superoxide dismutase activity in the rat striatum. Brain Res, 1998. 813(1): p. 200-2.

182. Wongpaiboonwattana, W., et al., Oxidative stress induces hypomethylation of LINE-1 and hypermethylation of the RUNX3 promoter in a bladder cancer cell line. Asian Pac J Cancer Prev, 2013. 14(6): p. 3773-8.

183. Patchsung, M., et al., Long interspersed nuclear element-1 hypomethylation and oxidative stress: correlation and bladder cancer diagnostic potential. PLoS One, 2012. 7(5): p. e37009.

184. Giorgi, G., P. Marcantonio, and B. Del Re, LINE-1 retrotransposition in human neuroblastoma cells is affected by oxidative stress. Cell Tissue Res, 2011. 346(3): p. 383-91.

185. Kloypan, C., et al., LINE-1 hypomethylation induced by reactive oxygen species is mediated via depletion of S-adenosylmethionine. Cell Biochem Funct, 2015. 33(6): p. 375-85.

186. Nover, L., K.D. Scharf, and D. Neumann, Cytoplasmic heat shock granules are formed from precursor particles and are associated with a specific set of mRNAs. Mol Cell Biol, 1989. 9(3): p. 1298-308.

187. Carelli, S., et al., Cysteine and glutathione secretion in response to protein disulfide bond formation in the ER. Science, 1997. 277(5332): p. 1681-4.

188. Locigno, R. and V. Castronovo, Reduced glutathione system: role in cancer development, prevention and treatment (review). Int J Oncol, 2001. 19(2): p. 221-36.

189. Noctor, G. and C.H. Foyer, ASCORBATE AND GLUTATHIONE: Keeping Active Oxygen Under Control. Annu Rev Plant Physiol Plant Mol Biol, 1998. 49: p. 249-279.

190. Zitka, O., et al., Redox status expressed as GSH:GSSG ratio as a marker for oxidative stress in paediatric tumour patients. Oncol Lett, 2012. 4(6): p. 1247-1253.

191. Manders, E.M.M., F.J. Verbeek, and J.A. Aten, MEASUREMENT OF COLOCALIZATION OF OBJECTS IN DUAL-COLOR CONFOCAL IMAGES. Journal of Microscopy-Oxford, 1993. 169: p. 375-382.

192. Manders, E.M., et al., Dynamics of three-dimensional replication patterns during the S-phase, analysed by double labelling of DNA and confocal microscopy. J Cell Sci, 1992. 103 (Pt 3): p. 857-62.

ABSTRACT

THE ROLE OF LINE-1 TRANSPOSABLE ELEMENT IN METHAMPHETAMINE NEUROTOXICITY IN THE NEUROGENIC ZONES

by

DONGYUE YU

AUGUST 2017

Advisor: Dr. Anna Moszczynska

Major: Pharmaceutical Sciences

Degree: Master of Science

Methamphetamine (METH) is a widely abused psychostimulant, which can cause neurotoxicity in the striatum and hippocampus. Several epigenetic changes were identified after binge METH exposure, including histone modification, DNA methylation, and changes in miRNA levels. We have shown that binge METH increases expression and activity of Long INterspersed Element (LINE-1), a transposable element, in doublecortin-positive neurons within rat neurogenic zones. The goal of the present study was to identify which type(s) of cells show increases in LINE-1 following binge METH exposure, and determine whether binge METH-induced increases in LINE-1 are associated with cell death. To achieve this goal, male adult Sprague Dawley rats were treated with binge METH (4x 10mg/kg, i.p.

every 2 h) or saline, sacrificed 24 hours later, and examined for LINE-1 expression and either markers of cell types in neurogenic zones or signs of apoptosis within the neurogenic zones. We found that increased LINE-1 expression co-localized with most GFAP-positive cells in both the subgranular zone (SGZ) and subventricular zone (SVZ), as well as most NeuN-positive cells in SGZ. We also found that LINE-1 expression co-localized with some, but not all, apoptotic marker expression within the neurogenic zones. However, LINE-1 expression did co-localize with an oxidative stress marker. Collectively, our data suggest that systemic administration of neurotoxic doses of binge METH increases the activity of LINE-1 mostly in glial cells and post-mitotic cells, and may be associated with responses to oxidative stress and/or gliosis. Supported by NIH/NIDA R01 DA034783

AUTOBIOGRAPHICAL STATEMENT

Name: DONGYUE YU

Education: 2017 M.S. Pharmaceutical Sciences, Wayne State University, Detroit, Michigan, U.S.A.

2015 B.S. Pharmacy, China Pharmaceutical University, Nanjing, Jiangsu, China.